

Figure 5 BF-227 staining in the temporal cortex (A), hippocampus (B) and cerebellum (C) of AD brain. In temporal and hippocampal brain sections, large numbers of amyloid plaques stained with BF-227. In contrast, no apparent staining was observed in the cerebellum. The stainability of BF-227 in the temporal cortex and hippocampus differed significantly from that in the cerebellum (D). * $P < 0.05$, one-way ANOVA followed by Scheffe's test.

changes in general behavior or bodyweight in male or female mice. During the 8 days of the experiment, no deaths occurred in any of the groups. This indicates that the dose for 50% lethality (LD_{50}) of i.v. administered BF-227 is higher than 10 mg/kg for male and female mice. In the subacute toxicity study, i.v. administration of BF-227 in tested doses did not produce any significant changes in general behavior or bodyweight in male or female mice. No significant differences in organ weight were observed between control and BF-227-administered groups. After the 14-day post-treatment period, mice did not show any microscopic alterations on pathological examination.

Discussion

Several research groups have worked to develop amyloid-imaging agents for use with PET. PIB is cur-

rently the most successful of these agents, showing high binding affinity for $A\beta$ fibrils and fast clearance from normal brain tissue.¹³ In the clinical trial, PIB-PET distinctly differentiated AD patients from normal individuals.⁴ Other amyloid-imaging agents, such as SB-13,¹⁴ IMPY¹⁵ and benzofuran derivatives,¹⁶ have also been explored for use as PET and single-photon emission computed tomography (SPECT) imaging probes. These agents display high binding affinity to $A\beta$ fibrils. The key chemical structure common to these imaging agents is an aminophenyl group, which is considered essential for binding to the β -pleated sheet structure of $A\beta$ fibrils. The present study, however, demonstrated that BF-227, a derivative of BF-168 with an aminothiazol group in place of the aminophenyl group, also binds strongly to amyloid- β fibrils. Furthermore, an autoradiographic study comparing BF-227 to BF-168 suggested that the aminothiazol group might contribute in a large way to

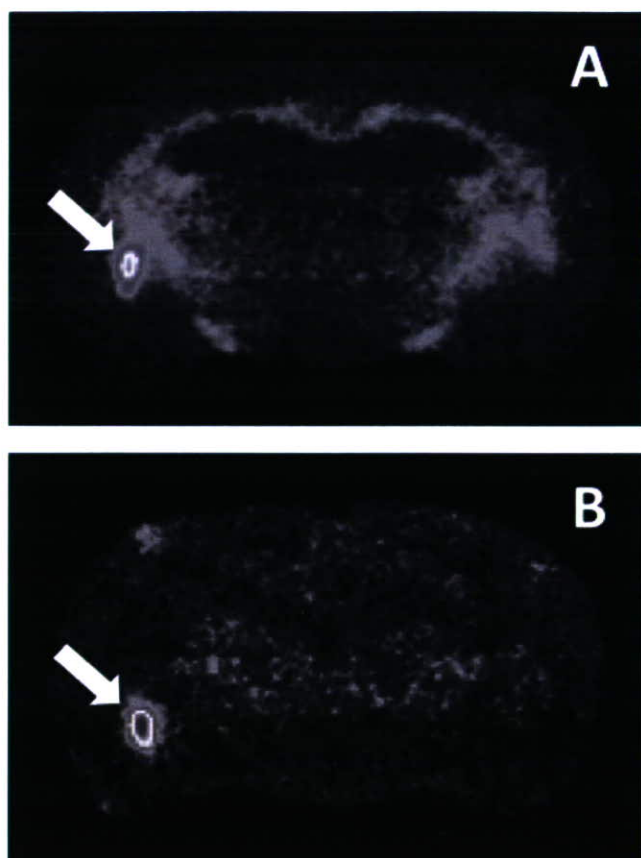


Figure 6 *In vivo* labeling of A β fibrils in brain sections from the A β -injected rat model with (^{18}F)BF-168 (A) and (^{18}F)BF-227 (B). Arrows indicate sites of A β injection.

decreased non-specific retention in normal brain tissue, particularly in white matter. This possibility should be examined in further studies, as this finding would be helpful in the design or modification of further series of amyloid-imaging agents.

Findings from the *in vitro* binding experiment indicated that the amount of BF-227 binding is proportional to the concentration of A β fibrils. Neuropathological findings also indicated that BF-227 preferentially binds to lesions containing dense A β fibrils. Densities of neuritic plaques are higher in the temporal, parietal and occipital lobes, moderate in the limbic lobe and lowest in the cerebellum.¹⁷ Our results for BF-227 stainability in different brain regions were consistent with this neuropathological pattern of A β deposition in AD patients. Brains from patients with AD are characterized by an anatomically widespread process of amyloid deposition. Presence of neuritic or cored plaques is considered the best indication of the presence of the disease process underlying AD.¹⁸ Quantitative measurement of A β fibril formation using BF-227 will thus allow discrimination of the disease process from normal aging processes. SP in the cerebellum are predominantly of the non-fibrillar type. The lack of obvious staining by BF-227 in the

cerebellum thus suggests the binding preference of this compound to fibrillar A β .

The present study demonstrated high binding affinity of BF-227 to fibrillar A β and preferential binding to SP in AD brain sections. *i.v.* administration of this compound into an A β -injected rat model demonstrated selective binding to amyloid fibrils in the brain and faster clearance from white matter than BF-168. The toxicity study indicated that BF-227 is safe for clinical use as a PET probe, with a very wide margin between the lethal dose of BF-227 (>10 mg/kg) and clinical dose in human PET studies (<100 ng/kg). Considering all these findings together, BF-227 appears applicable for use as an *in vivo* amyloid-imaging agent. We are currently engaging in a clinical PET trial using ^{11}C -labeled BF-227 in AD patients.¹⁹ This trial will elucidate the clinical utility of BF-227 in humans.

Acknowledgments

This study was partially supported by the Novartis Foundation for Gerontological Research, the Special Coordination Funds for Promoting Science and Technology, the Program for the Promotion of Fundamental Studies in Health Science by the National Institute of Biomedical Innovation, the Industrial Technology Research Grant Program from the New Energy and Industrial Technology Development Organization (NEDO) of Japan, Health and Labor Sciences Research Grants for Translational Research from the Japanese Ministry of Health, Labor and Welfare, a JST grant on research and education in molecular imaging, and an Astrazeneca Research Grant.

References

- 1 Price JL, Morris JC. Tangles and plaques in nondemented aging and "preclinical" Alzheimer's disease. *Ann Neurol* 1999; **45**: 358–368.
- 2 Nordberg A. PET imaging of amyloid in Alzheimer's disease. *Lancet Neurol* 2004; **3**: 519–527.
- 3 Klunk WE, Wang Y, Huang GF, Debnath ML, Holt DP, Mathis CA. Uncharged thioflavin-T derivatives bind to amyloid-beta protein with high affinity and readily enter the brain. *Life Sci* 2001; **69**: 1471–1484.
- 4 Klunk WE, Engler H, Nordberg A *et al.* Imaging brain amyloid in Alzheimer's disease with Pittsburgh Compound-B. *Ann Neurol* 2004; **55**: 306–319.
- 5 Agdeppa ED, Kepe V, Liu J *et al.* Binding characteristics of radiofluorinated 6-dialkylamino-2-naphthylethylidene derivatives as positron emission tomography imaging probes for beta-amyloid plaques in Alzheimer's disease. *J Neurosci* 2001; **21**: RC189.
- 6 Small GW, Kepe V, Ercoli LM *et al.* PET of brain amyloid and tau in mild cognitive impairment. *N Eng J Med* 2006; **355**: 2652–2663.
- 7 Okamura N, Suemoto T, Shimadzu H *et al.* Styrylbenzoxazole derivatives for *in vivo* imaging of amyloid plaques in the brain. *J Neurosci* 2004; **24**: 2535–2541.

- 8 Shimadzu H, Suemoto T, Suzuki M *et al.* Novel probes for imaging amyloid- β : F-18 and C-11 labeling of 2-(4-aminostyryl) benzoxazole derivatives. *J Label Compd Radiopharm* 2004; **47**: 181–190.
- 9 Okamura N, Suemoto T, Shiomitsu T *et al.* A novel imaging probe for in vivo detection of neuritic and diffuse amyloid plaques in the brain. *J Mol Neurosci* 2004; **24**: 247–255.
- 10 Suemoto T, Okamura N, Shiomitsu T *et al.* In vivo labeling of amyloid with BF-108. *Neurosci Res* 2004; **48**: 65–74.
- 11 Paxinos G, Watson C. *The Rat Brain in Stereotaxic Coordinates*. San Diego, CA: Academic Press, 1998.
- 12 Mathis CA, Klunk WE. Imaging β -amyloid plaques and neurofibrillary tangles in the aging human brain. *Curr Pharm Design* 2004; **10**: 1469–1492.
- 13 Mathis CA, Wang Y, Holt DP, Huang GF, Debnath ML, Klunk WE. Synthesis and evaluation of ^{11}C -labeled 6-substituted 2-arylbenzothiazoles as amyloid imaging agents. *J Med Chem* 2003; **46**: 2740–2754.
- 14 Verhoeff NP, Wilson AA, Takeshita S *et al.* In-vivo imaging of Alzheimer disease beta-amyloid with [^{11}C]SB-13 PET. *Am J Geriatr Psychiatry* 2004; **12**: 584–595.
- 15 Kung MP, Hou C, Zhuang ZP *et al.* Characterization of IMPY as a potential imaging agent for β -amyloid plaques in double transgenic PSAPP mice. *Eur J Nucl Med Mol Imaging* 2004; **31**: 1136–1145.
- 16 Ono M, Kawashima H, Nonaka A *et al.* Novel benzofuran derivatives for PET imaging of β -amyloid plaques in Alzheimer's disease brain. *J Med Chem* 2006; **49**: 2725–2730.
- 17 Arnold SE, Hyman BT, Flory J, Damasio AR, Van Hoesen GW. The topographical and neuroanatomical distribution of neurofibrillary tangles and neuritic plaques in the cerebral cortex of patients with Alzheimer's disease. *Cereb Cortex* 1991; **1**: 103–116.
- 18 Price JL. Diagnostic criteria for Alzheimer's disease. *Neurobiol Aging* 1997; **18**: S67–S70.
- 19 Kudo Y, Okamura N, Furumoto S *et al.* 2-[2-(2-dimethylaminothiazol-5-yl) ethenyl]-6-[2-(fluoro) ethoxy]benzoxazole: a novel PET imaging agent for in vivo detection of dense amyloid plaques in Alzheimer's disease patients. *J Nucl Med* 2007; **48**: 553–561.

Imaging Amyloid Pathology in the Living Brain

Nobuyuki Okamura^{a,*}, Shozo Furumoto^b, Hiroyuki Arai^c, Ren Iwata^d, Kazuhiko Yanai^a and Yukitsuka Kudo^b

^aDepartment of Pharmacology, Tohoku University School of Medicine, Sendai 980-8575, Japan, ^bTohoku University Biomedical Engineering Research Organization (TUBERO), Sendai 980-8575, Japan, ^cCenter for Asian Traditional Medicine, Department of Geriatrics and Gerontology, Tohoku University School of Medicine, Sendai 980-8574, Japan, ^dDivision of Radiopharmaceutical Chemistry, Cyclotron and Radioisotope Center, Tohoku University, Sendai 980-8578, Japan

Abstract: Progressive deposition of amyloid plaques in the brain, which begins before the appearance of cognitive decline, is an initiating event in the pathogenesis of Alzheimer's disease. Therefore, noninvasive detection of amyloid pathology is important for presymptomatic diagnosis and preventive therapy for Alzheimer's disease. Recent research advances have enabled the *in vivo* imaging of amyloid pathology in humans using nuclear medicine technology. Several amyloid-binding agents have been developed and evaluated by positron emission tomography (PET) and single photon emission computed tomography (SPECT) for their use as contrast agents. Available clinical evidence indicates that amyloid imaging enables the early diagnosis of Alzheimer's disease with high accuracy and suggests its usefulness for the prediction of progression to Alzheimer's disease in subjects with mild cognitive impairment and probably also in cognitively normal individuals. Another application of this technology is as a surrogate marker for monitoring brain amyloid. In this review, we describe recent progress in the development of amyloid imaging technology and human clinical trials.

Keywords: Amyloid, Alzheimer's disease, Positron emission tomography (PET), molecular imaging, senile plaque, neurofibrillary tangle.

INTRODUCTION

Alzheimer's disease (AD) is the most common cause of dementia in the elderly. The definitive diagnosis of AD relies on postmortem assessment, with characteristic pathological changes such as neuron death, senile plaques (SPs), and neurofibrillary tangles (NFTs). Currently, the amyloid cascade hypothesis is widely accepted to account for the pathogenesis of AD [1]. SP is mainly composed of amyloid β ($A\beta$), which is generated by proteolytic reaction of β and γ -secretase from the amyloid precursor protein (APP). In this hypothesis, the mismetabolism of APP is the initiating event in AD pathogenesis. Excessive generation of $A\beta$ causes aggregation of $A\beta$ and the formation of SPs, and this is followed by the formation of NFTs, neuron death, neurotransmitter deficit, and cognitive decline. If this hypothesis is correct, optimal therapeutic strategies for interrupting the disease process should be directed toward modifying the generation, clearance, and cytotoxicity of $A\beta$.

Early diagnosis and treatment of AD is important in maintaining the patient's activities of daily living as long as possible and preventing the patient from becoming bedridden. A notable feature of AD is a discrepancy between clinical symptoms and pathological findings in the brain (Fig. (1)). Even in the clinically early stage of dementia, a large amount of SP is already present in the brain [2, 3]. These changes in the brain probably start 10–20 years before clinical symptoms appear. Therefore, if the deposition of SPs in the brain can be measured noninvasively, subjects who are

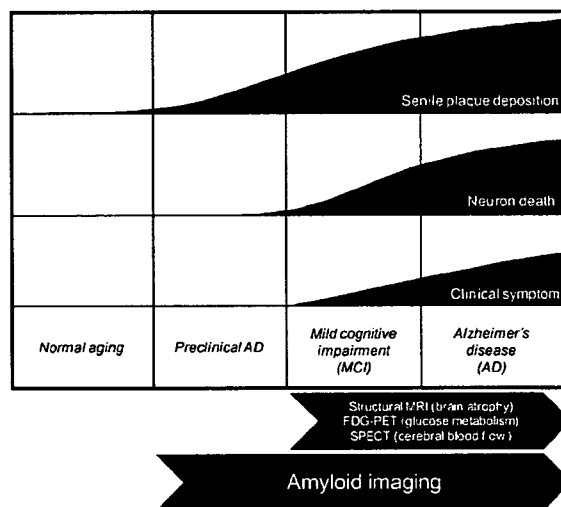


Fig. (1). Senile plaque deposition, neuron death and clinical symptom of Alzheimer's disease.

certain to develop AD (i.e., "preclinical AD") could be screened as candidates for preventive therapy.

Recently, several imaging techniques, including positron emission tomography (PET), single photon emission computed tomography (SPECT), magnetic resonance imaging, and near-infrared imaging, have been developed for the noninvasive detection of SPs in AD patients. These techniques, recently classified as "amyloid imaging", are considered ideal for screening candidates for anti-amyloid therapy. PET is the most popular method for amyloid

*Address correspondence to this author at the Department of Pharmacology, Tohoku University School of Medicine, 2-1, Seiryomachi, Aoba-ku, Sendai 980-8575, Japan; Tel: + 81-22-717-8058; Fax: +81-22-717-8060; E-mail: oka@mail.tains.tohoku.ac.jp

imaging, because of its advantages of high sensitivity, good spatial resolution, quantitative results, and ease of probe development.

DEVELOPMENT OF AMYLOID-IMAGING AGENTS

Recent advances in molecular imaging have enabled the noninvasive detection of amyloid deposits by PET or SPECT. For the high-contrast detection of amyloid deposits, imaging agents should have high binding affinity for A β fibrils and substantial permeability through the blood-brain barrier (BBB). Several amyloid-binding agents have been developed for the *in vivo* detection of amyloid deposits (Fig. (2)). The development of these agents started with the use of Congo red, which is commonly used for the histochemical staining of amyloid [4]. However, the BBB permeability of Congo red is limited because of its molecular size and electrostatic charge. Therefore, several Congo red derivatives have been developed with improved BBB permeability without reduced binding to amyloid [5-8]. Chrysamine-G is the first Congo red derivative that has been examined as an *in vivo* amyloid-imaging probe. However, entry of this compound into the brain is limited. Other derivatives, including BSB, ISB, and methoxy-X04, have also been developed to improve the BBB permeability. BSB successfully visualizes brain amyloid deposits in APP-transgenic mice after intravenous administration of the

compound. However, this compound has insufficient BBB permeability for it to be useful as a clinical PET tracer. The first successful amyloid imaging agent to have been administered to humans is 2-(1-{6-[(2-¹⁸F]fluoroethyl)(methyl)amino]-2-naphthyl}ethylidene)malononitrile (¹⁸F)FDDNP [9]. One of the characteristics of this agent is its ability to bind both SPs and NFTs in the AD brain. In addition, this compound is extremely lipophilic; therefore, it can penetrate the BBB more easily than previously reported compounds [10]. Interestingly, this compound binds to the same site in A β fibrils as non-steroidal anti-inflammatory drugs (NSAIDs) do. Therefore, this agent enables us to determine the occupancy rate of NSAIDs and experimental drugs in SPs [11]. Other candidate amyloid-imaging agents include thioflavin-T derivatives [12, 13]. N-methyl-[¹¹C]2-(4'-methylaminophenyl)-6-hydroxybenzothiazole ([¹¹C]PIB) is one such derivative and is currently the most successful amyloid-imaging agent. This compound shows high binding affinity for A β fibrils and SPs in AD brain homogenates, in contrast to low binding affinity for NFTs [14]. After intravenous administration, this agent shows high BBB permeability and rapid washout from normal brain tissue. Other amyloid-imaging agents, such as IMPY, stilbene, benzofuran, and acridine orange derivatives, have also been explored for use as PET and SPECT imaging probes [15-19]. The iodinated agent IMPY has been explored as a SPECT

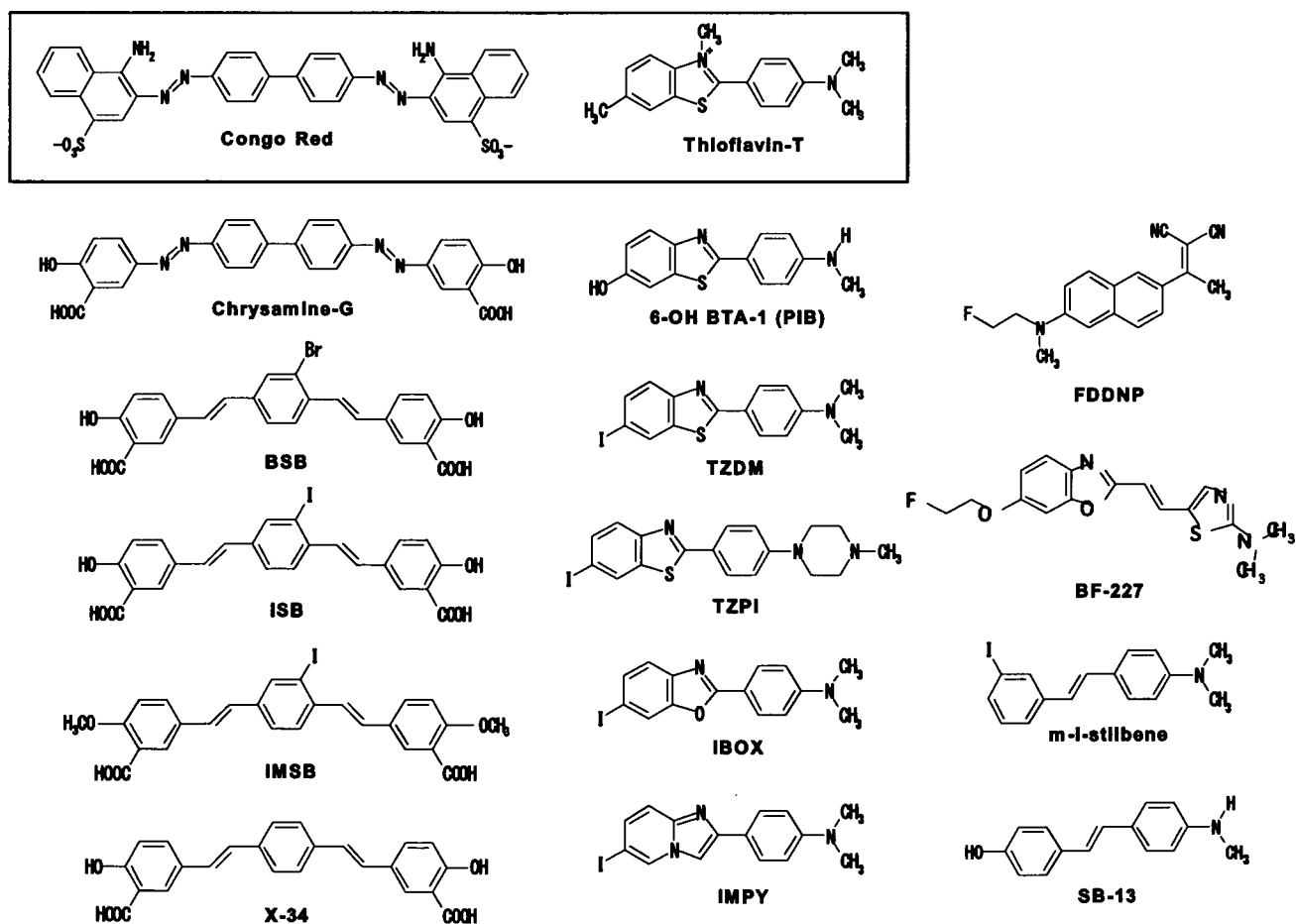


Fig. (2). Chemical structures of common imaging probes for amyloid plaques.

imaging agent and has been used in humans. Other iodinated agents are also under evaluation.

Benoxazole derivatives are other possible amyloid-imaging agents [20-23]. Their chemical structures, binding affinities for A β fibrils, and pharmacokinetic data are summarized in Table 1. Most of these compounds show high binding affinity for both A β 1-40 and A β 1-42 fibrils. BF-191 and BF-208, which have halogens as substituents for amino groups, show low affinity for both A β 1-40 and A β 1-42 fibrils, suggesting that amino groups have a crucial role in binding to A β fibrils. All compounds have good BBB permeability. BF-227 shows faster washout from normal brain tissue than the other compounds [23, 24]. BF-227 distinctly stained SPs during the neuropathological staining of AD brain sections, and this staining pattern correlated well with A β immunostaining (Fig. (3)). Fluorescence microscopy revealed that this agent binds preferentially to SPs rather than NFTs. An acute and subacute toxicity study of BF-227 indicated sufficient safety for clinical use as a PET probe.

HUMAN PET STUDY

Human amyloid imaging was first studied using [^{18}F]FDDNP [9]. A [^{18}F]FDDNP PET study revealed regional accumulation of [^{18}F]FDDNP in the SP- and NFT-rich areas of the brain [25]. Global FDDNP-PET binding distinctly differentiated AD patients from normal subjects. FDDNP retention in the medial temporal lobes of subjects with mild cognitive impairment (MCI) was intermediate between levels in AD patients and normal control subjects. This finding is consistent with the observation in an autopsy study that the concentration of NFTs in the medial temporal lobes was intermediate between that in normally aging subjects and AD patients [26]. These binding characteristics indicate that this imaging agent is useful in tracing the progression of AD from the MCI stage. In addition, this agent has the potential to differentiate atypical prion disease from AD [27]. The weakness of this agent is the low signal-to-background ratio of the images, which is due to the considerable amount of nonspecific accumulation in normal brain tissue [28].

In comparison with [^{18}F]FDDNP, [^{11}C]PIB PET images differentiated AD patients from normal individuals more distinctly [29]. PIB retention was observed in the SP-rich neocortex of the brain but not in the NFT-rich medial temporal cortex, indicating that this agent binds selectively to SPs. A quantitative imaging method using PIB has already been validated [30, 31]. Over half the subjects with MCI also showed neocortical PIB accumulation to the same level as AD patients [32, 33]. Interestingly, MCI subjects who at clinical follow-up converted to AD showed higher PIB retention than subjects with non-progressive MCI, indicating that neocortical PIB retention is a marker for the prediction of progression to AD in the MCI stage [34]. A PIB-PET study in a nondemented population revealed elevated cortical retention of PIB in four nondemented persons [35]. These nondemented PIB-positive cases additionally showed an abnormality in the concentration of A β 1-42 in cerebrospinal fluid, suggesting the presence of SPs in the absence of cognitive impairment [36]. There was a strong relationship between impaired memory performance and PIB binding in

the nondemented population [37]. These findings suggest that amyloid imaging may be sensitive enough for the detection of a preclinical AD state. However, one should be careful when assessing abnormalities in the distribution of PIB, because PIB retention is also observed in cerebral amyloid angiopathy [38, 39]. Amyloid imaging may be useful as a surrogate marker for monitoring brain amyloid deposition during anti-amyloid therapy. However, longitudinal PIB-PET evaluation indicated relatively stable PIB retention after 2 years of follow-up in AD patients, suggesting that brain amyloid deposition reflected by PIB retention reaches a plateau at the early clinical stages of AD [40]. Therefore, therapy that retards the synthesis of A β (e.g., β - and γ -secretase inhibitors) should be started before the retention of amyloid-imaging tracers reaches a plateau.

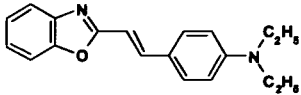
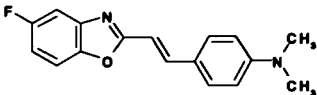
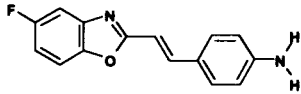
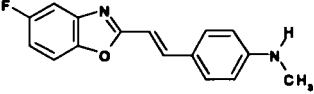
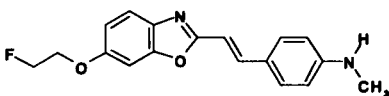
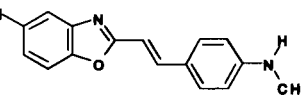
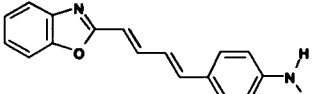
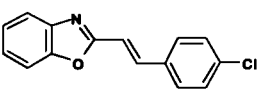
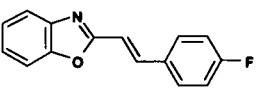
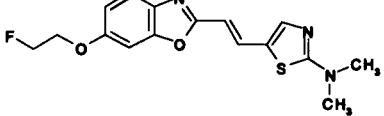
The stilbene derivative SB-13 has also been used in a human PET study [41]. In a PET study, [^{11}C]SB-13 exhibited similar binding properties to PIB. For expanded use in clinical investigations, an [^{18}F]labeled stilbene derivative is under investigation.

A PET study using [^{11}C]BF-227 was performed at Tohoku University [23]. Neocortical retention of BF-227 was observed in an AD patient (Fig. (4)). A subject with MCI also showed cortical retention of BF-227. Interestingly, this subject was confirmed to progress to AD during the follow-up period, suggesting that cortical retention of BF-227 indicates a high risk of conversion to AD in MCI subjects. Several MCI subjects showed a distribution of BF-227 similar to that in normally aged subjects. All Alzheimer's patients and about 60% of MCI subjects showed an elevated standardized uptake value (SUV) ratio in the neocortical regions. Even in MCI subjects showing prominent retention of BF-227, the neocortical SUV ratio was below the mean value observed in AD patients. This finding suggests that MCI is a pathologically transitional state between normal aging and dementia, and that the amyloid deposition reflected by BF-227 retention does not reach a plateau in the MCI stage. Voxel-by-voxel analysis of BF-227 PET images demonstrated higher retention of BF-227 in the temporoparietal region in AD patients [23]. The pattern of distribution resembles the distribution of neuritic plaques in postmortem AD brains [42, 43]. Microscopic observation also indicates preferential binding of BF-227 to neuritic plaques in AD brain sections (Fig. (3)). In an *in vitro* binding experiment, BF-227 binding to A β increased linearly with increasing A β fibril formation [24]. For these reasons, BF-227 is considered to bind neuritic plaques selectively *in vivo*. A validation study is required to determine whether the retention of BF-227 in the neocortex accurately reflects the level of neuritic plaques rather than the level of diffuse plaques.

FUTURE DIRECTION OF PROBE DEVELOPMENT

The commercialization of [^{18}F]labeled agents or SPECT imaging agents is necessary for the wide clinical application of amyloid imaging. Because of the limited half-life of [^{11}C] (20 min), the supply of [^{11}C]labeled PET agents is limited to facilities with an on-site cyclotron. [^{18}F]labeled agents are generally easier for routine clinical use because of the longer half-life of [^{18}F] (110 min). Currently, several [^{18}F]labeled agents for amyloid imaging are under clinical evaluation. To

Table 1. Binding Affinity of Benzoxazole Derivatives for A β Fibrils and Brain Uptakes After Intravenous Administration in Normal Mice

Compounds	Chemical structure	Kd or Ki (nM)		Brain uptake (%ID/g)	
		A β 1-40	A β 1-42	2 min	30 min
BF-125		1.5 \pm 0.76	4.9 \pm 1.9	3.0 \pm 0.87	3.0 \pm 0.53
BF-133		2.1 \pm 1.1	3.4 \pm 0.73	5.5 \pm 0.40	3.8 \pm 0.030
BF-140		4.7 \pm 2.2	2.1 \pm 0.18	5.5 \pm 0.60	1.1 \pm 0.076
BF-145		3.0 \pm 0.46	4.5 \pm 1.9	4.4 \pm 1.80	1.6 \pm 0.40
BF-168		2.5 \pm 2.3	6.4 \pm 1.0	3.9 \pm 0.22	1.6 \pm 0.0071
BF-180		6.8 \pm 1.4	10.6 \pm 1.5	2.4 \pm 0.52	1.8 \pm 0.010
BF-185		2.5 \pm 2.3	14 \pm 10	3.9 \pm 0.49	3.8 \pm 0.16
BF-191		> 5000	> 5000	12 \pm 0.26	1.7 \pm 0.16
BF-208		> 5000	> 5000	5.6 \pm 0.64	0.28 \pm 0.024
BF-227		1.8 \pm 0.42	4.3 \pm 1.5	7.9 \pm 0.18	0.54 \pm 0.029

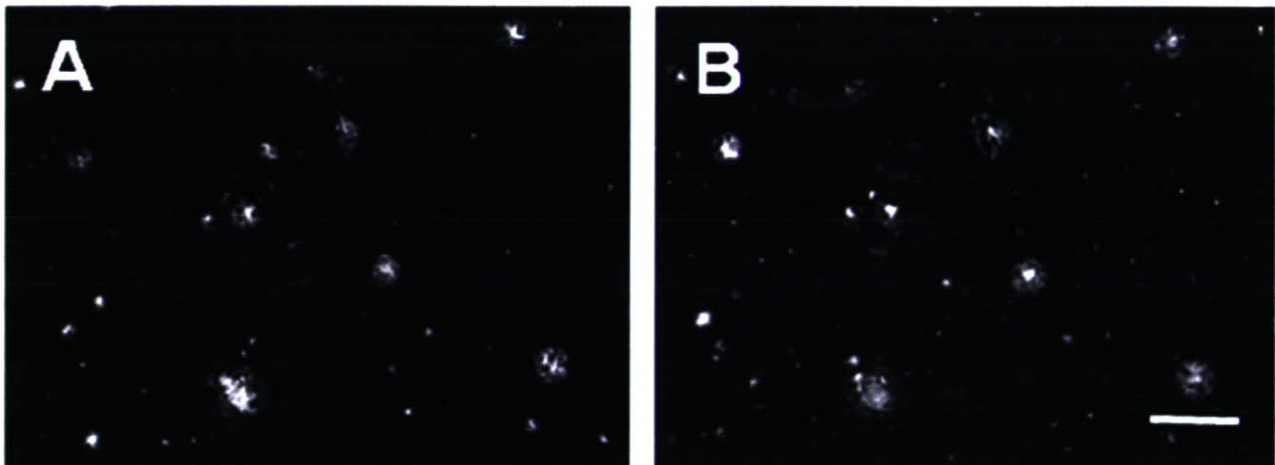


Fig. (3). Fluorescence microscopic images of senile plaques in Alzheimer's disease using BF-227 (A) and A β specific antibody 6F/3D (B) Bar = 100 μ m.

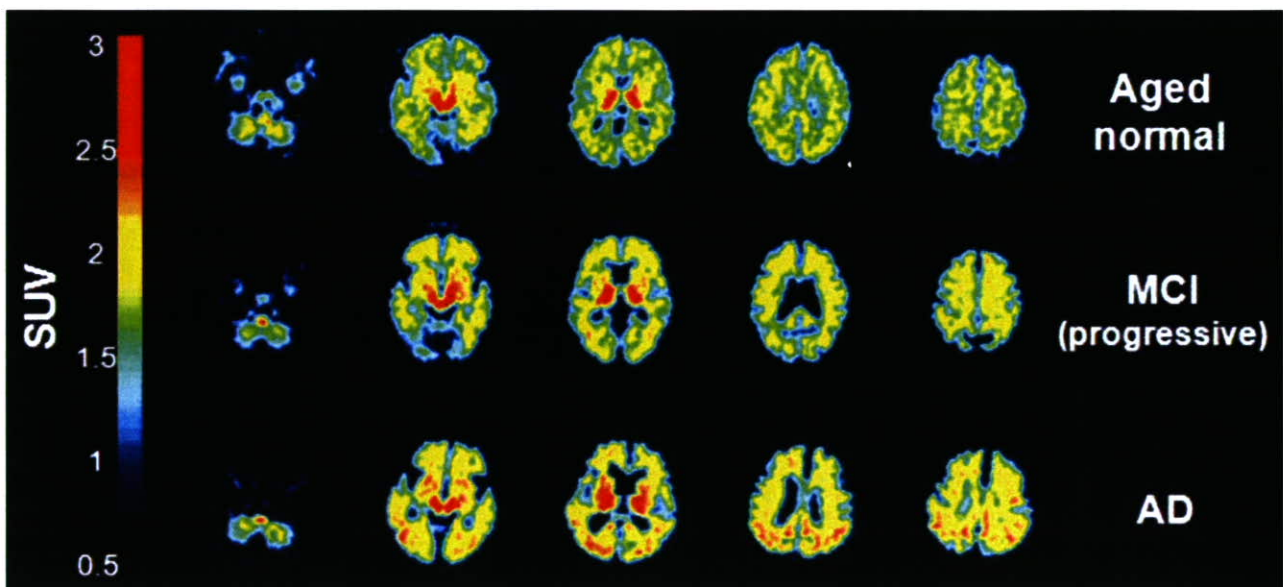


Fig. (4). Mean SUV images between 20 and 40 min post-injection of [^{11}C]BF-227 in aged normal, MCI and AD cases.

obtain a better understanding of the pathophysiology of AD, it is also necessary to visualize the distributions of A β pathology and tau pathology individually. However, no surrogate markers are available for evaluating the deposition of NFTs in the brain, because of the difficulty in developing a tau-specific imaging probe [44]. We previously introduced the novel compounds BF-126 and BF-170 as candidates for tau imaging [45]. In AD brain sections, BF-126 and BF-170 visualize NFTs, neuropil threads, and PHF-type neuritis distinctly. For clinical application, optimization of these compounds to reduce non-specific binding is in progress.

CONCLUSION

Several amyloid-imaging agents have been successfully developed for PET imaging. These agents displayed high binding affinity for A β fibrils and high BBB permeability. [^{11}C]PIB, [^{18}F]FDDNP, and [^{11}C]BF-227 displayed selective

in vivo binding to amyloid in the brain and clearly differentiated early AD patients from normal populations. The development of ^{18}F -labeled agents or SPECT imaging agents is necessary for the wide application of amyloid imaging. The development of an NFT-specific imaging agent is also much needed. Amyloid imaging is currently the best method for the early and accurate diagnosis of AD and for monitoring amyloid pathology in the brain. This imaging technology and the forthcoming anti-amyloid therapy will cooperatively contribute to the prevention of dementia.

ACKNOWLEDGEMENTS

This study was partially supported by the Special Coordination Funds for Promoting Science and Technology, the Program for the Promotion of Fundamental Studies in Health Science of the National Institute of Biomedical Innovation, the Industrial Technology Research Grant

Program of the New Energy and Industrial Technology Development Organization (NEDO) of Japan, Health and Labour Sciences Research Grants for Translational Research from the Japanese Ministry of Health, Labour and Welfare, and a JST grant for research and education in molecular imaging.

DISCLOSURE STATEMENT

All authors have no conflict of interest.

REFERENCES

- [1] Tanzi RE, Bertram L. Twenty years of the Alzheimer's disease amyloid hypothesis: a genetic perspective. *Cell* 2005; 120: 545-555.
- [2] Goldman WP, Price JL, Storandt M, *et al.* Absence of cognitive impairment or decline in preclinical Alzheimer's disease. *Neurology* 2001; 56: 361-367.
- [3] Price JL, Morris JC. Tangles and plaques in nondemented aging and "preclinical" Alzheimer's disease. *Ann Neurol* 1999; 45: 358-368.
- [4] Klunk WE, Debnath ML, Pettegrew JW. Development of small molecule probes for the beta-amyloid protein of Alzheimer's disease. *Neurobiol Aging* 1994; 691-698.
- [5] Klunk WE, Debnath ML, Pettegrew JW. Chrysin-G binding to Alzheimer and control brain: autopsy study of a new amyloid probe. *Neurobiol Aging* 1995; 16: 541-548.
- [6] Skovronsky DM, Zhang B, Kung MP, Kung HF, Trojanowski JQ, Lee VM. *In vivo* detection of amyloid plaques in a mouse model of Alzheimer's disease. *Proc Natl Acad Sci USA* 2000; 97: 7609-7614.
- [7] Zhuang ZP, Kung MP, Hou C, *et al.* Radioiodinated styrylbenzenes and thioflavins as probes for amyloid aggregates. *J Med Chem* 2001; 44: 1905-1914.
- [8] Klunk WE, Bacskai BJ, Mathis CA, *et al.* Imaging Abeta plaques in living transgenic mice with multiphoton microscopy and methoxy-X04, a systemically administered Congo red derivative. *J Neuropathol Exp Neurol* 2002; 61: 797-805.
- [9] Shoghi-Jadid K, Small GW, Agdeppa ED, *et al.* Localization of neurofibrillary tangles and beta-amyloid plaques in the brains of living patients with Alzheimer disease. *Am J Geriatr Psychiatry* 2002; 10: 24-35.
- [10] Agdeppa ED, Kepe V, Liu J, *et al.* Binding characteristics of radiofluorinated 6-dialkylamino-2-naphthylethylidene derivatives as positron emission tomography imaging probes for beta-amyloid plaques in Alzheimer's disease. *J Neurosci* 2001; 21: RC189.
- [11] Agdeppa ED, Kepe V, Petri A, *et al.* *In vitro* detection of (S)-naproxen and ibuprofen binding to plaques in the Alzheimer's brain using the positron emission tomography molecular imaging probe 2-(1-[6-[(2-[(18F]fluoroethyl)(methyl) amino]-2-naphthyl]ethylidene)malononitrile. *Neuroscience* 2003; 117: 723-730.
- [12] Mathis CA, Wang Y, Klunk WE. Imaging beta-amyloid plaques and neurofibrillary tangles in the aging human brain. *Curr Pharm Des* 2004; 10: 1469-1492.
- [13] Klunk WE, Wang Y, Huang GF, Debnath ML, Holt DP, Mathis CA. Uncharged thioflavin-T derivatives bind to amyloid-beta protein with high affinity and readily enter the brain. *Life Sci* 2001; 69: 1471-1484.
- [14] Klunk WE, Wang Y, Huang GF, *et al.* The binding of 2-(4'-methylaminophenyl)benzothiazole to postmortem brain homogenates is dominated by the amyloid component. *J Neurosci* 2003; 23: 2086-2092.
- [15] Kung MP, Hou C, Zhuang ZP, *et al.* IMPY: an improved thioflavin-T derivative for *in vivo* labeling of beta-amyloid plaques. *Brain Res* 2002; 956: 202-210.
- [16] Kung HF, Kung MP, Zhuang ZP, *et al.* Iodinated tracers for imaging amyloid plaques in the brain. *Mol Imaging Biol* 2003; 5: 418-426.
- [17] Ono M, Wilson A, Nobrega J, *et al.* ¹¹C-labeled stilbene derivatives as Abeta-aggregate-specific PET imaging agents for Alzheimer's disease. *Nucl Med Biol* 2003; 30: 565-571.
- [18] Ono M, Kawashima H, Nonaka A, *et al.* Novel benzofuran derivatives for PET imaging of beta-amyloid plaques in Alzheimer's disease brains. *J Med Chem* 2006; 49: 2725-2730.
- [19] Suemoto T, Okamura N, Shiomitsu T, *et al.* *In vivo* labeling of amyloid with BF-108. *Neurosci Res* 2004; 48: 65-74.
- [20] Okamura N, Suemoto T, Shimadzu H, *et al.* Styrylbenzoxazole derivatives for *in vivo* imaging of amyloid plaques in the brain. *J Neurosci* 2004; 24: 2535-2541.
- [21] Okamura N, Suemoto T, Shiomitsu T, *et al.* A novel imaging probe for *in vivo* detection of neuritic and diffuse amyloid plaques in the brain. *J Mol Neurosci* 2004; 24: 247-255.
- [22] Furumoto S, Okamura N, Iwata R, Yanai K, Arai H, Kudo Y. Recent advances in the development of amyloid imaging agents. *Curr Top Med Chem* 2007; 7: 1773-1789.
- [23] Kudo Y, Okamura N, Furumoto S, *et al.* 2-(2-[2-Dimethylaminothiazol-5-yl]ethenyl)-6-(2-[fluoro]ethoxy)benzoxazole: a novel PET agent for *in vivo* detection of dense amyloid plaques in Alzheimer's disease patients. *J Nucl Med* 2007; 48: 553-561.
- [24] Okamura N, Furumoto S, Funaki Y, *et al.* Binding and safety profile of novel benzoxazole derivative for *in vivo* imaging of amyloid deposits in Alzheimer's disease. *Geriatr Gerontol Int* 2007 (in press)
- [25] Small GW, Kepe V, Ercoli LM, *et al.* PET of brain amyloid and tau in mild cognitive impairment. *N Engl J Med* 2006; 355: 2652-2663.
- [26] Petersen RC, Parisi JE, Dickson DW, *et al.* Neuropathologic features of amnesic mild cognitive impairment. *Arch Neurol* 2006; 63: 665-672.
- [27] Boxer AL, Rabinovici GD, Kepe V, *et al.* Amyloid imaging in distinguishing atypical prion disease from Alzheimer disease. *Neurology* 2007; 69: 283-290.
- [28] Bacskai BJ, Klunk WE, Mathis CA, Hyman BT. Imaging amyloid-beta deposits *in vivo*. *J Cereb Blood Flow Metab* 2002; 22: 1035-1041.
- [29] Klunk WE, Engler H, Nordberg A, *et al.* Imaging brain amyloid in Alzheimer's disease with Pittsburgh Compound-B. *Ann Neurol* 2004; 55: 306-319.
- [30] Price JC, Klunk WE, Lopresti BJ, *et al.* Kinetic modeling of amyloid binding in humans using PET imaging and Pittsburgh Compound-B. *J Cereb Blood Flow Metab* 2005; 25: 1528-1547.
- [31] Lopresti BJ, Klunk WE, Mathis CA, *et al.* Simplified quantification of Pittsburgh Compound B amyloid imaging PET studies: a comparative analysis. *J Nucl Med* 2005; 46: 1959-1972.
- [32] Rowe CC, Ng S, Ackermann U, *et al.* Imaging beta-amyloid burden in aging and dementia. *Neurology* 2007; 68: 1718-1725.
- [33] Kempainen NM, Aalto S, Wilson IA, *et al.* PET amyloid ligand [¹¹C]PIB uptake is increased in mild cognitive impairment. *Neurology* 2007; 68: 1603-1606.
- [34] Forsberg A, Engler H, Almkvist O, *et al.* PET imaging of amyloid deposition in patients with mild cognitive impairment. *Neurobiol Aging* 2007 (in press)
- [35] Mintun MA, Larossa GN, Sheline YI, *et al.* [¹¹C]PIB in a nondemented population: potential antecedent marker of Alzheimer disease. *Neurology* 2006; 67: 446-452.
- [36] Fagan AM, Mintun MA, Mach RH, *et al.* Inverse relation between *in vivo* amyloid imaging load and cerebrospinal fluid Abeta42 in humans. *Ann Neurol* 2006; 59: 512-519.
- [37] Pike KE, Savage G, Villemagne VL, *et al.* Beta-amyloid imaging and memory in non-demented individuals: evidence for preclinical Alzheimer's disease. *Brain* 2007; 130: 2837-2844.
- [38] Bacskai BJ, Frosch MP, Freeman SH, *et al.* Molecular imaging with Pittsburgh Compound B confirmed at autopsy: a case report. *Arch Neurol* 2007; 64: 431-434.
- [39] Johnson KA, Gregas M, Becker JA, *et al.* Imaging of amyloid burden and distribution in cerebral amyloid angiopathy. *Ann Neurol* 2007; 62: 229-234.
- [40] Engler H, Forsberg A, Almkvist O, *et al.* Two-year follow-up of amyloid deposition in patients with Alzheimer's disease. *Brain* 2006; 129: 2856-2866.
- [41] Verhoeff NP, Wilson AA, Takeshita S, *et al.* In-vivo imaging of Alzheimer disease beta-amyloid with [¹¹C]SB-13 PET. *Am J Geriatr Psychiatry* 2004; 12: 584-595.
- [42] Arnold SE, Hyman BT, Flory J, Damasio AR, Van Hoesen GW. The topographical and neuroanatomical distribution of neurofibrillary tangles and neuritic plaques in the cerebral cortex of patients with Alzheimer's disease. *Cereb Cortex* 1991; 1: 103-116.
- [43] Cummings JL, Cole G. Alzheimer disease. *JAMA* 2002; 287: 2335-2338.

- [44] Small GW, Agdeppa ED, Kepe V, Satyamurthy N, Huang SC, Barrio JR. *In vivo* brain imaging of tangle burden in humans. *J Mol Neurosci* 2002; 19: 323-327.
- [45] Okamura N, Suemoto T, Furumoto S, *et al.* Quinoline and benzimidazole derivatives: candidate probes for *in vivo* imaging of tau pathology in Alzheimer's disease. *J Neurosci* 2005; 25: 10857-10862.

Received: December 5, 2007

Revised: December 7, 2007

Accepted: December 10, 2007

Recent Advances in the Development of Amyloid Imaging Agents

Shozo Furumoto^{a*}, Nobuyuki Okamura^b, Ren Iwata^c, Kazuhiko Yanai^b, Hiroyuki Arai^d and Yukitsuka Kudo^a

^aBiomedical Engineering Research Organization, Tohoku University, Sendai 980-8575, Japan, ^bDepartment of Pharmacology, Tohoku University School of Medicine, Sendai 980-8575, Japan, ^cDivision of Radiopharmaceutical Chemistry, Cyclotron and Radioisotope Center, Tohoku University, Sendai 980-8578, Japan, ^dDepartment of Geriatrics and Gerontology, Tohoku University School of Medicine, Sendai 980-8575, Japan

Abstract: Excessive amyloid- β (A β) deposition in the brain is one of the most crucial events in the early pathological stage of Alzheimer's disease (AD). Therefore, A β deposits have enough potential to become a useful biomarker for not only an early diagnosis of AD, but also for the assessment of the clinical efficacy of anti-A β therapies, if they can be measured non-invasively and reliably in living patients. As a potent candidate technique to measure this biomarker, PET amyloid imaging using a radioligand for A β deposits has received much attention. A large number of A β ligands have been synthesized and evaluated as candidates for amyloid imaging agents. These can be classified into six categories of derivatives: Congo-red, Thioflavine T, stilbene, vinylbenzoxazole, DDNP, and miscellaneous. Many of these derivatives exhibit high binding affinities to A β fibrils (below 20 nM) and some of them also show excellent brain pharmacokinetic profiles. The concept of amyloid imaging is currently being tested in human PET studies using optimized amyloid imaging agents. Despite the small number of subjects, these studies have demonstrated sufficiently promising results. This review article provides an overview of recent advances in the development of amyloid imaging agents, and includes: a summary of the fundamental basis and clinical significance of amyloid imaging; lists of binding affinity data for 135 compounds classified into 12 molecular frameworks; a comprehensive discussion of the *in vitro* and *in vivo* features of representative A β ligands; and a discussion of the current state of clinical evaluation of these amyloid imaging agents (PIB, SB-13, BF-227, and FDDNP).

Keywords: Alzheimer's disease, amyloid imaging, radioligand, PIB, SB-13, BF-227, FDDNP.

1. INTRODUCTION

Alzheimer's disease (AD) is a neurodegenerative disorder clinically characterized by a progressive impairment in cognitive function and behavior, and is the most common form of dementia particularly in elderly [1-4]. It has been estimated that approximately 1% of those aged 60-64 years is affected by AD. The prevalence of AD, however, shows an almost exponential increase with age (doubling approximately every 5 years) after age 60, reaching 20% to 40% of the population over the age 85 [5,6]. The number of patients is predicted to rise in the future due to the expected increase in life expectancy. In terms of social costs, AD is one of the most expensive diseases because it requires not only medication, but also caregiving over a long period [7].

Since the most consistent neurochemical abnormality associated with AD is a severe loss of cholinergic neurons in the areas of the brain related to memory and learning, the current therapeutic approaches are mainly based on the use of acetylcholinesterase inhibitors to preserve brain cholinergic nerve function [8]. This approach can help to prevent some symptoms from becoming worse or to bring modest symptomatic improvements in some patients, but it can not halt the pathological progress of AD. Accordingly, without the advent of appropriate and effective therapies for AD, serious public health problems and the social cost of the disease is expected to increase substantially in the future. That is, there is an enormous medical need for the development of novel therapeutic strategies for AD.

In recent years, great efforts have been made to study the underlying pathogenic mechanisms in AD and translate research advances into the development of new classes of drugs and biomarkers [9-11]. The most widely accepted theory regarding the pathogenic process of AD is the amyloid cascade hypothesis [12-14], which explains that the accumulation and aggregation of amyloid- β (A β) peptide in the brain trigger a pathological cascade ultimately leading to neuronal degeneration and dementia. Hence, the major focus of drug development for AD treatment has been directed toward modifying the pathology through lowering the A β level in the brain [15-17].

With the advances in drug development, new biomarkers that can be used for the early diagnosis of AD and clinical evaluation of the disease-modifying drugs targeting A β have become increasingly important [18-20]. Based on the amyloid cascade theory, A β deposits in the AD brain are probably the most relevant biomarker. Currently, *in vivo* amyloid imaging techniques that can non-invasively and reliably assess A β deposition using a tracer that binds to A β fibrils have received much attention for their promise in imaging this biomarker [21-25]. A large number of radiotracers have been developed for positron emission tomography (PET) and single-photon emission computed tomography (SPECT) during the past decade [26-29], and some of these have entered into preliminary clinical studies in recent years [29,30].

In this article, we first describe AD pathology, focusing on the amyloid cascade hypothesis, and discuss anti-amyloid therapy for the treatment of AD and the need for biomarkers for AD diagnosis and therapy, leading to a deeper understanding of the fundamental basis and clinical significance of amyloid imaging. We then review amyloid imaging agents, discussing the requirements for tracer development and the compounds that have been reported to date. Finally, we provide an overview of the current state of clinical evaluation of amyloid imaging agents.

2. AD PATHOLOGY AND THE AMYLOID CASCADE HYPOTHESIS

The neuropathological hallmarks of AD are neuritic plaques (NPs) and neurofibrillary tangles (NFTs) in the medial temporal lobe structures and cortical areas of the brain together with selective neuronal and synaptic loss [11,31,32]. NPs, extracellular lesions, consist of a central core of aggregated A β peptides [33] surrounded by dystrophic neurites, reactive astrocytes and activated microglia. NFTs represent intracellular bundles of paired helical filaments that are composed of the microtubule-associated protein tau in an abnormally hyperphosphorylated form [34]. Deposition of NPs precedes NFT formation and is relatively specific for AD [13], whereas NFTs are also found in other neurodegenerative disorders [35,36]. While both lesions are indispensable prerequisites for a definitive diagnosis of AD, more attention has focused on the role of A β in the pathogenesis of AD. Although the exact mechanisms leading to the development of AD have not been elucidated completely, A β is assumed to fulfill a causal role in the pathology of AD (Fig. (1)). This so-called amyloid cascade hypothesis is

*Address correspondence to this author at Biomedical Engineering Research Organization, Tohoku University, 2-1, Seiryō-cho, Aoba-ku, Sendai 980-8575, Japan; Tel: +81-22-717-7586; Fax: +81-22-717-7586; E-mail: shozo@tubero.tohoku.ac.jp

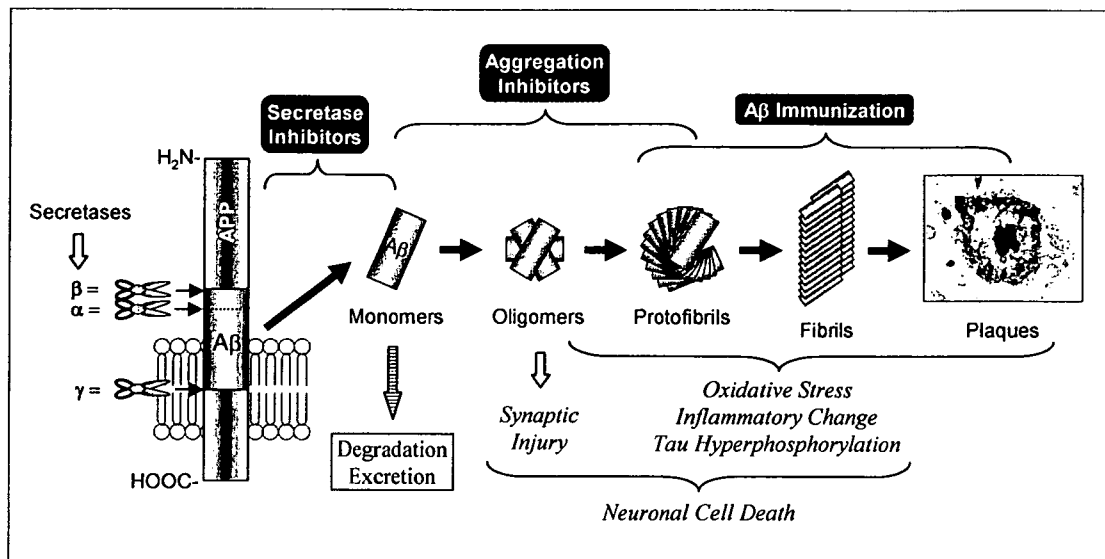


Fig. (1). Schematic illustration of the A β amyloid cascade from APP cleavage by secretases to generate A β monomers, to plaque formation, via oligomers, protofibrils, and fibrils. Causative factors for neuronal injury are indicated in italic letters under the A β pathway. Anti-amyloid agents are also shown in solid-white letters above the therapeutic targets in the A β pathway.

widely accepted as the most plausible theory for understanding the pathogenesis of AD.

A β is produced from a large membrane-spanning glycoprotein, termed β -Amyloid Precursor Protein (APP) [37], through abnormal sequential cleavages made by proteinases referred to as secretases [38,39]. During the normal processing of APP, namely the non-amyloidogenic pathway, α -secretase first cleaves within the A β domain of APP to generate soluble carboxyl-truncated forms of APP, and γ -secretase cleaves the remnant C-terminal proteolytic products further to yield non-amyloidogenic fragments. In the alternative, amyloidogenic pathway, β -secretase instead of α -secretase cleaves APP at the N-terminal site of A β , and then γ -secretase cleaves the C-terminal site to release A β [40-42]. Although the resulting A β peptide varies from 39 to 43 amino acids in length, the main forms of A β involved in AD pathology are the shorter 40 amino acid form (A β 40) and the longer 42 amino acid form (A β 42). In particular, A β 42 is the predominant A β species found in amyloid plaques in patients with AD, while A β 40 is the main species of A β secreted normally from cells. A β 42 tends to polymerize and subsequently aggregates more rapidly than A β 40 [43]; these properties are thought to be associated with both an early onset of AD and an increased risk for AD.

A β is produced continuously in the brains of both healthy individuals and AD patients. Under physiological conditions, the A β level is tightly controlled by efflux to blood [44] and cerebrospinal fluid (CSF) and proteolytic degradation by amyloid-degrading enzymes, such as insulin-degrading enzyme and neprilysin [45]. The amyloid cascade hypothesis holds that certain pathogenic factors cause an imbalance between the production and clearance of A β , leading to a progressive accumulation of A β , in particular of A β 42 peptide [46], in the brain, triggering a cascade of amyloidogenic events as follows. Soluble A β excessively accumulated in the brain undergoes a conformational change to acquire a high β -sheet content, stimulating the aggregation of A β peptides into soluble oligomers, which have been implicated to impair neuronal and synaptic function by altering membrane permeability [47-49]. These oligomers aggregate further into insoluble fibrils and eventually into immature and amorphous forms of plaques termed diffuse plaques, which are believed to represent the initial phase of

plaque formation. These aggregations cause neuronal injury through the induction of oxidative stress [50], inflammatory responses (microglial and astrocytic activation) [51], and abnormal tau hyperphosphorylation, resulting in selective neuronal loss, neurotransmitter deficits, and cognitive symptoms.

The strong evidence for the amyloid cascade hypothesis derives from studies of gene mutations in APP [52] and presenilin-1 and -2 [53], proteins that form the catalytic unit of the γ -secretase protein complex [40]. These various gene mutations all lead to increased levels of A β 42 and plaque formation in the brain, and all represent a similar clinical entity recognized as an early-onset form of familial Alzheimer's disease (FAD). People with Down's syndrome, who carry an extra copy of the APP gene, also produce higher levels of A β from birth, and almost invariably develop amyloid deposits after the age of 30 years [54]. In addition, several studies using transgenic animal models afford convincing supportive evidence for the amyloid cascade theory [55,56]. In one of the most successful models of AD, triple transgenic model mice (3xTg-AD: PS1M146V, APP^{swe} and TauP301L) develop A β plaques prior to NFT pathology with a temporal and regional specific profile that closely resembles pathological development in the human brain, including synaptic dysfunction, induction of inflammatory processes, and neurodegeneration [57,58].

Taken together, considerable evidence from a variety of pathological, biochemical, and genetic studies points to A β and the process of amyloid deposition, even if not the amyloid deposits themselves, as the upstream causative factor of the pathogenesis of AD.

3. ANTI-AMYLOID THERAPY

According to the amyloid cascade theory, disease-modifying therapy for AD is expected to be performed through lowering the level of A β in the brain. Thus, many of the current therapeutic approaches are directed at reducing A β accumulation in the brain by modifying different points in the A β pathway (amyloid cascade), such as A β /APP proteolytic processing, A β aggregation, and A β clearance.

Because A β originates from APP through sequential proteolytic cleavages by β - and γ -secretases, inhibition or modulation of these

enzymes have been prime therapies used to lower the A β level [59-61]. γ -Secretase inhibitors such as LY450139 reduce the production of both A β 40 and A β 42 [62], while γ -secretase modulators such as FlurizanTM lower A β 42 production by selectively modulating, but not inhibiting, γ -secretase activity, to shift the cleavage of APP away from A β 42 production [63]. At present, LY450139 and FlurizanTM are being evaluated in human clinical Phase II and III trials, respectively.

Preventing the formation and deposition of A β fibrils represents another promising approach to developing disease-modifying drugs. AlzhemedTM, a glycosaminoglycan mimic that binds to soluble A β , is one of the most advanced drugs that inhibits A β fibrilization, and is currently under clinical evaluation in Phase III trials [64].

As an alternative strategy that targets A β directly, antibody-mediated A β clearance or removal from the brain also has potential for reducing A β accumulation in the brain. Active immunization with the A β immuno-conjugate ACC-001, which is composed of an N-terminal fragment of A β and a carrier protein, and passive immunization with the humanized monoclonal antibody AAB-001 are now undergoing clinical trials [65].

Collectively, several drug candidates designed to modify amyloidogenic processes in the early stages of Alzheimer's amyloid pathology are currently under clinical evaluation. For the appropriate evaluation of drug efficacy, there is an essential need for biomarkers that indicate whether drugs are actually altering the underlying degenerative process. In addition, appropriate biomarkers for the early diagnosis of AD are also required, because anti-amyloid therapy should be started as early as possible after the initiation of amyloid pathology to obtain an optimum therapeutic effect and to delay or halt the clinical outcomes.

4. AMYLOID IMAGING

Since AD is a progressive neurodegenerative disorder leading to the death of neurons that cannot be replaced once lost, an early diagnosis is critical for physicians, patients and their families to make early social, legal, and medical decisions about treatment and care. Early treatment with even current medications, starting before neurodegeneration becomes too severe and widespread, may provide greater benefits over the long term [66,67]. Moreover, early diagnosis and treatment of AD are expected to contribute substantially to social and financial savings. Consequently, a considerable effort has been made in the last decade to identify reliable biomarkers of AD for disease detection at an early stage [18,68].

At present, clinical diagnosis of AD is generally performed by evaluation of the progressive impairment of cognitive functions and

exclusion of other causes of dementia. A definitive diagnosis of AD can only be made by postmortem observation of NPs and NFTs in brain sections; this is regarded as the gold standard [69,70]. This means that, according to current clinical diagnostic criteria, AD can not be diagnosed before the disease has progressed so far that clinical outcomes have appeared. Recent studies have demonstrated that PET imaging of glucose metabolism and CSF biomarkers (total tau, phosphorylated tau, and A β 42) show preliminary promise for the identification of AD traits [68,71]. Both methods indicate a high predictive value for the identification of preclinical AD in patients with mild cognitive impairment (MCI), which is suggestive of the earliest symptomatic stage of AD but is insufficient to fulfill traditional diagnostic criteria for AD [72]. However, postmortem studies have revealed that some cognitively intact individuals and many patients with MCI already carry a heavy burden of AD-like neuropathology [73-75]. The pathogenic processes, especially the formation of NPs, are estimated to start a few decades before clinical symptoms become evident (Fig. (2)). Considering this fact along with the amyloid cascade hypothesis, A β deposits in the brain are a reasonable and promising biomarker for the early diagnosis of AD.

To detect A β burden in the brain, much attention has been directed toward amyloid imaging, which enables the spatial distribution and degree of deposition of A β in the brain to be visualized non-invasively using a ligand that binds to A β fibrils. This *in vivo* imaging measurement would have great value as a diagnostic marker for identifying individuals with incipient AD in the MCI stage, and even those in the presymptomatic phase of the disease. Amyloid imaging would allow us to investigate the pathogenic role of A β in AD pathology by following and relating directly the pathological progression and cognitive decline in the same individuals over time.

In addition, amyloid imaging is expected to serve as a useful tool for the clinical assessment of disease-modifying therapeutics targeting the A β pathway, making it possible to evaluate whether the level of A β deposits in the brain is lowered by the drug; namely, whether the drugs actually exert their action against their targets [22,76,77]. Such *in vivo* evaluation of drug influences on disease targets would provide convincing proof of the mechanism. Furthermore, selection of appropriate subjects who have A β deposits in their brains, but intact cognition, using amyloid imaging, would be a rational strategy for clinical trials of such disease-modifying therapeutics. Measurement of A β deposition by amyloid imaging may be more reliable than measurement of standard clinical or cognitive outcomes in large clinical trials, thereby increasing the power to detect a small effect and reducing sample size.

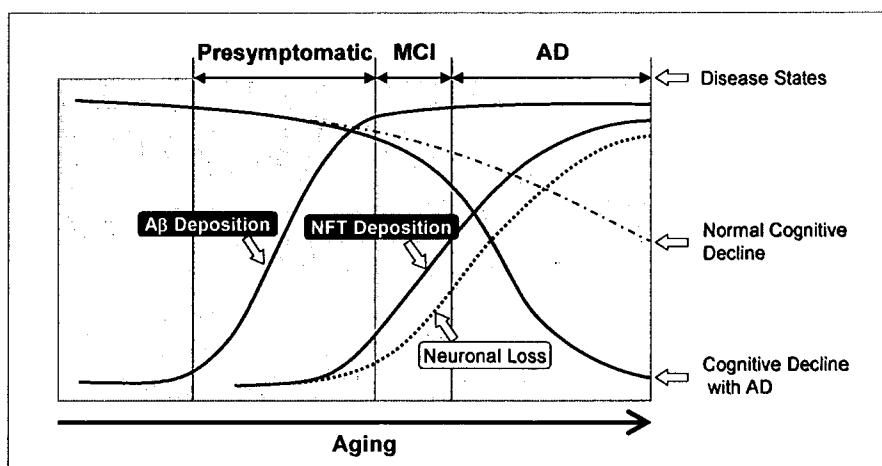


Fig. (2). Hypothetical model of the neuropathological progression (A β and NFT depositions) and clinical outcomes in Alzheimer's disease.

Development of amyloid imaging agents, including probes for PET, SPECT, Magnetic Resonance Imaging [78-80], and near-infrared fluorescence imaging [81], have advanced rapidly during the last decade. Among these, PET radioligands have been the most extensively studied, and a significant number of candidates have been reported to date. Some of these have proceeded to exploratory clinical evaluations and promising results have been achieved in amyloid imaging studies.

5. AMYLOID IMAGING AGENTS

5.1. Requirements for Amyloid Imaging Agents

In general, development of PET radioligands starts with finding a "seed" compound, which binds to the target molecule. The chemical structure is then optimized to have appropriate features for imaging the target. With regard to amyloid imaging, the radioligand requires several criteria for optimization, including that it shows: high binding affinity for A β fibrils; high blood-brain barrier (BBB) permeability with appropriate lipophilicity; and excellent brain pharmacokinetics with rapid brain uptake and fast clearance from the normal brain without non-specific binding.

The binding affinity required for radioligands is generally considered in relation to the total concentration of the target molecule. The concentrations of A β in the AD brain have been reported to be 1-10 μ M [82], and these levels are considerably higher than those of typical neuroreceptors or transporters (1-200 nM) [83]. Therefore, the requisite binding affinities (K_d; the equilibrium dissociation constant) for amyloid imaging agents have been set as below 20 nM [84], which is relatively higher than those of neuroreceptors or transporters in the range between 10 pM and 1 nM [83]. As an alternative indicator, inhibition constant (K_i) is also often used for evaluating binding affinities due to its utility in the efficient screening of a number of non-radiolabeled candidates; this value is required to achieve the same level as the K_d.

Showing a high BBB permeability via passive diffusion, a radioligand for amyloid imaging should be a small molecule with a molecular weight (MW) of less than 400-500 [85]. In addition, the radioligand should be lipophilic enough to cross the BBB easily, but not so lipophilic as to cause unacceptable binding to plasma proteins and non-specific binding to normal brain tissue. A parabolic relationship has been demonstrated between radiotracer brain uptake and its Log P value, an octanol-water partition coefficient used as a parameter of lipophilicity, showing the uptake peak between a Log P of 2 and 3 [86,87]. The appropriate Log P value for brain entry has been suggested to be in the range between 1 and 3 [88].

Because of the short half-lives of positron emitters (¹¹C, 20.4 min; ¹⁸F, 109.8 min), intravenously injected radioligand should be incorporated rapidly into the brain and, after reaching the peak level of uptake, non-specific bound or free radioligand should be cleared fast in the half-life time equal to or less than that of the radioactive decay of the radionuclide [27,89]. For this purpose, binding affinity, MW, and lipophilicity of radioligands are comprehensively optimized to afford desirable pharmacokinetic properties leading to adequate images with a high signal-to-noise ratio suitable for quantitative analysis of ligand binding potency.

5.2. Biomolecules

Some biomolecules such as antibodies or A β peptide itself were explored in the search of amyloid imaging agents, because they bind specifically to A β amyloid and plaques *in vitro* [90-94]. However, these molecules do not possess the appropriate properties for brain amyloid imaging *in vivo* studies. One of the most serious problems is their low BBB permeability due to their large MW. Although many attempts have been made to improve their BBB permeability (brain uptake) by modifying their structure or applying a drug delivery system, no promising results have yet been

achieved. Therefore, over the past decade, an alternative approach for developing amyloid imaging agents, based on small organic compounds, has been taken.

5.3. Congo Red Analogues

Congo red (CR) is an organic dye molecule widely used for the histological staining of amyloid especially in postmortem pathological studies of AD. Klunk and coworkers evaluated quantitatively CR binding to amyloid-like proteins with a β -sheet conformation [95]. They speculated that the key structural feature of CR is the two acidic functional groups and the space between them. Since CR possesses low lipophilicity (Log P = -0.18) owing to two highly charged amino-naphthalene sulfonic acid groups in the structure, Klunk and coworkers investigated the binding potential of Chrysamine G (CG), a lipophilic analogue of CR, which also has two acidic functional groups with the same amount of space between them as seen in CR.

CG showed high binding affinity to synthetic A β aggregates (K_i = 2.7 nM), and total binding of [¹⁴C]CG to homogenates of AD brains was nearly three times as high as that of age-matched control brains [27,96,97]. However, brain uptake of [¹⁴C]CG in mice was limited. Thus, considerable efforts to develop CG derivatives with high BBB permeability were expended through modifying the structure to afford a low MW and relatively high lipophilicity, resulting in a new series of CG analogues (1-8) with a new pharmacophore, bis-styryl benzene (styrylbenzene), indicated as Framework A in Fig. (4).

Methoxy-X04 (8; Me-X04), an optimized CG derivative, has a lower MW (344), lacking the carboxylic acid groups, is moderately lipophilic (Log P = 2.6), and exhibits selective binding to A β plaques in postmortem AD brain sections and PS1/APP Tg mouse brain [27,98]. Interestingly, removing the carboxylic acid groups had little effect on the binding affinity for A β aggregates and A β plaques, indicating that the acidic functional group is not a predominant factor in the binding mechanism. Moreover, removal of the carboxylic acid groups leaving only the weakly acidic phenols resulted in a neutral form of Me-X04 at physiologic pH (pK_a = 10.8), and thereby, the brain uptake of [¹¹C]Me-X04 was shown to be 7-fold higher than that of the related carboxylic acid derivative Me-X34 (7) [98]. Nevertheless, the level of brain uptake of the optimized compound was still insufficient for using in human PET studies.

The styrylbenzene framework was also used by other researchers for the development of amyloid imaging agents such as ISB, IMSB, and so on [99-101]. Although [¹²⁵I]ISB (10) and [¹²⁵I]IMSB (11) showed high binding affinity to A β aggregates, their BBB permeabilities were very low, probably due to their carboxylic acid groups. If the carboxylic acid groups were removed from ISB and IMSB, the brain uptake of the resultant derivatives would be expected to increase, but not to exceed the level of Me-X04 uptake, because of their relatively high MW.

Since the framework of styrylbenzene is so rigid that further optimization of the derivatives is limited, recent research has shifted to the usage of different types of molecular framework for developing amyloid imaging agents.

5.4. Thioflavin-T Analogues

Thioflavin T (ThT) and Thioflavin S (ThS) are other organic dyes often used for histopathological staining of amyloid plaques (Fig. (3)). Although ThS is more widely used in *in vitro* histological staining studies, ThT is a more attractive seed compound for developing amyloid imaging agents, because of its relatively low MW and well-defined chemical structure [102]. However, ThT contains a positively charged benzothiazolium unit, whose ionic charge is unfavorable for brain uptake. Therefore, the development of amyloid imaging agents based on ThT requires chemical modification of the charged structure to generate a neutral form.

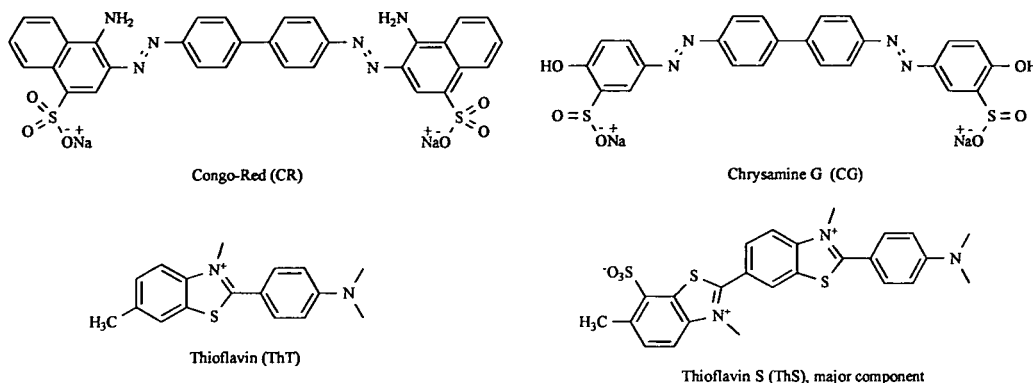


Fig. (3). Organic dye molecules widely used for the histological staining of amyloid.

Klunk and co-workers developed a series of neutral ThT derivatives (13-25, 30-32) containing uncharged benzothiazole instead of benzothiazolium for PET imaging [84,103-105]. That is, the molecular framework in the derivatives can be represented as Framework B in Fig. (4), where X and Y are "S" and "N", respectively. They systematically evaluated the binding affinities and lipophilicities of the derivatives, and investigated the relationship between the lipophilicity and brain entry or clearance of the derivatives in detail [84]. As a result, all of the neutral derivatives showed higher binding affinities (K_i : 2-64 nM) for A β 40 aggregates than the charged parent compound, ThT (K_i : 580 nM). Additionally, an interesting correlation was observed between $\log P_{C18}$ and the clearance as expressed by the 2 min-to-30 min ratio, indicating that the least lipophilic compounds tended to be cleared from the brain the fastest, while the most lipophilic ones were retained for over 30 min [84]. Based on the brain clearance property, compound 20 (PIB), which showed rapid clearance from normal mouse (2 min-to-30 min ratio = .116) and baboon brain, was finally selected as a promising candidate for further biological evaluation. An *in vitro* binding study using [3 H]PIB and AD brain homogenates indicated a high binding affinity with K_d value of 2.5 nM [106].

Kung and co-workers also independently developed 2-arylbenzothiazole derivatives as neutral ThT derivatives (35, TZDM; 36, TZPI) for SPECT imaging [100]. These derivatives showed specific binding to A β 40 and A β 42 aggregates at subnanomolar concentrations. Using [125 I]TZDM and [125 I]M5B in a competitive binding assay, these authors clearly demonstrated that there are distinctive and mutually exclusive binding sites on A β 40 and A β 42 aggregates for 2-arylbenzothiazole derivatives and styrylbenzene derivatives. Kung and co-workers have continued to develop a variety of ThT derivatives containing benzoxazole (37, IBOX) [107], benzofuran (47-54) [108,109] or imidazopyridine (100-104), in the place of benzothiazolium. Among them, a benzofuran derivative [11 C]50 showed potential for *in vivo* amyloid imaging: high binding affinity (K_i : 0.7 nM) for A β and good brain clearance (2 min-to-30 min ratio = 13.6). An imidazopyridine derivative [125 I]100 known as IMPY also demonstrated desirable characteristics for *in vivo* imaging of A β plaques [110-114].

As related F-18-labeled compounds, 2-(4-fluorophenyl)benzothiazole derivatives (33, 34) [115,116] and ThT derivatives containing benzothiophene (38-46) [117] or imidazopyridine (105-108) [118,119] instead of benzothiazolium were also reported by other research groups. The benzothiophene derivatives exhibited excellent binding affinities for A β aggregates (K_i : 0.2-4.3 nM) and high initial brain uptake, but very slow clearances from normal brain tissue relative to PIB and 50. However, their slow clearances would be improved by introducing a hydroxy group into the benzene ring of benzothiophene to reduce their lipophilicities, as in

the case of PIB and 50. For F-18-labeled IMPY analogues ([18 F]105, [18 F]106, [18 F]108), PET studies of brain pharmacokinetics in mice and rhesus monkeys showed moderately favorable profiles; however, further improvements are needed to reduce radioactive metabolites and/or increase binding affinity.

5.5. Stilbene and Related Derivatives

Stilbene, represented as Framework C in Fig. (4), where X is "C", is a simple but potent pharmacophore belonging to A β binding ligands that were found by Kung and co-workers in a search for a new A β probe [120,121]. While the stilbene skeleton is a partial structure of styrylbenzene, an *in vitro* binding assay revealed that the binding affinities of stilbene derivatives toward styrylbenzene binding sites were very low. By contrast, stilbene derivatives showed high binding affinities to the binding sites of TZDM (35), a ThT derivative, especially in the case of aromatic rings containing an electron-donating group, such as *p*-amino, *p*-methoxy, or *p*-hydroxy groups [120]. Consequently, a series of simple stilbene derivatives with 4-amino and 4'-hydroxy substitution groups (58-63) were screened as possible PET imaging agents [122]. Although all of the stilbenes displayed high binding affinities (K_i : 1-6 nM), compound 61 (SB-13) was selected as a lead compound for C-11 labeling and further biological evaluation because of its moderate lipophilicity. As expected, [11 C]SB-13 showed very good brain penetration and clearance from normal rat brain after i.v. injection. In addition, *in vitro* autoradiography demonstrated specific binding of [11 C/ 3 H]SB-13 to A β deposits in the tissue sections from transgenic AD model mouse brain and AD brain [114]. [3 H]SB-13 displayed high-affinity binding to AD brain homogenates with a K_d value of 2.4 nM. These results suggested that simple stilbene derivatives like [11 C]SB-13 might have potential for visualizing A β deposits in the brain using PET.

Kung and co-workers then designed and synthesized stilbene derivatives (69, 71, 73) containing a 2-fluoromethylpropan-1-ol structure aiming at F-18-labeled amyloid imaging agents [123]. These compounds exhibited high binding affinities in a competitive binding assay using [125 I]IMPY and AD brain homogenates. Biological evaluations using their F-18-labeled compounds clarified that [18 F]73 ([18 F]FMAPO) shows the most preferable features: excellent brain penetration (9.75 %ID/g at 2 min); rapid brain washout (0.72 %ID/g at 60 min); and specific binding to amyloid plaques in AD brain homogenates and sections. However, the increasing bone uptake of radioactivity with time, reaching 7.8 %ID/g at 2 hr postinjection, indicates that the defluorination of [18 F]FMAPO is likely to occur *in vivo* [123].

Another series of F-18 labeled stilbene derivatives ([18 F]64-[18 F]67) was also developed by Kung and co-workers [124]. Fluorinated polyethylene glycol (PEG) units ($n=2-5$) were attached to stilbene derivatives on the 4'-hydroxy group of SB-13 to lower

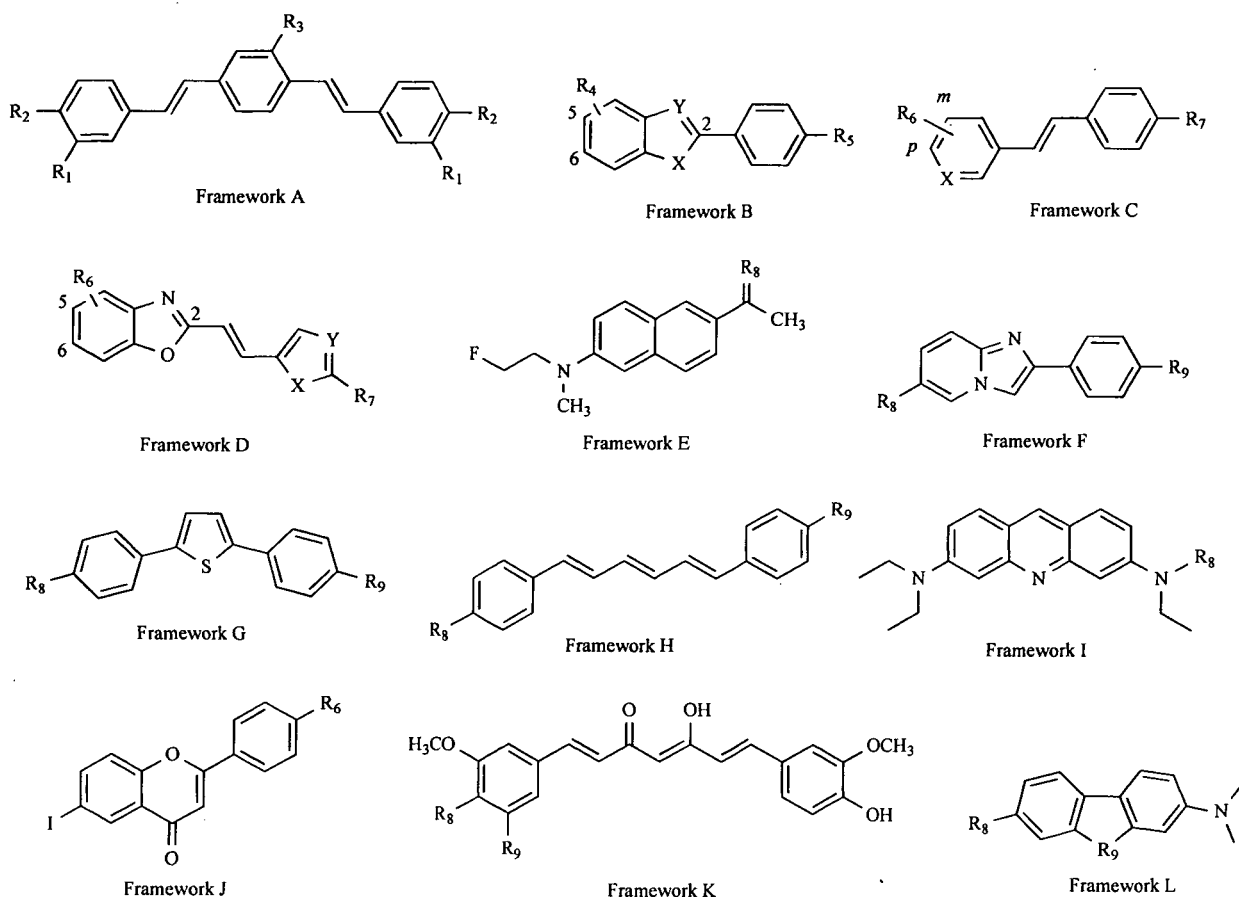


Fig. (4). Molecular frameworks of A β ligands that have been reported to date. Each substitution (R₁-R₉) is indicated in Tables 1 ~ 4.

the lipophilicity and improve bioavailability. The addition of a fluorinated PEG group had little effect on the high binding affinity and the moderate lipophilicity of the parent stilbene derivative. Consequently, these fluorinated PEG stilbene derivatives indicated high binding affinities for amyloid plaques and good pharmacokinetic properties. While defluorination of these derivatives was also detected in the biodistribution studies, the bone uptake values were relatively low (1.5-2.8 %ID/g) in comparison to [¹⁸F]FMAPO and related derivatives.

These fluorinated PEG units were introduced to other types of amyloid ligands including PIB, IMPY, BF-168 (**89**) and styrylpyridine derivatives (**80-82**) [125]. These derivatives (**26-29**, **77-79**, **95-97**, **109-113**), containing fluorinated PEG, displayed the same degree of binding affinities as the corresponding parent compounds [126,127]. PIB derivatives (**26-29**) showed moderately favorable brain pharmacokinetics in the case of shorter PEG length ($n=2$), but high bone uptake was simultaneously observed. IMPY derivatives (**109-113**) exhibited low brain uptake and slow brain clearance. Styrylpyridine derivatives (**77-79**) [127], having the same framework of stilbene, displayed high binding affinities for amyloid plaques and preferable brain kinetics, similar to FMAPO.

5.6. Vinylbenzoxazole Derivatives

The vinylbenzoxazole derivatives, indicated as Framework D in Fig. (4), were recently reported by Kudo and co-workers as promising candidate amyloid imaging agents (**83-94**) [128-131]. These derivatives contain not only a benzoxazole and an aromatic ring in their structures, like ThT derivatives, but also a double bond between them, like stilbene derivatives. A competitive binding

assay using [¹²⁵I]**93** (BF-180) and synthetic A β aggregates indicated sufficiently high binding affinities for use as A β ligands. Although the molecular size of the 2-vinylbenzoxazole derivatives is slightly larger than that of ThT and stilbene derivatives, these three types of derivatives appear to share a common binding site on A β aggregates, because the 2-vinylbenzoxazole derivative **89** (BF-168) and the related analogue 2-(4-dimethylaminostyryl)benzothiazole inhibit the binding to A β of [¹²⁵I]IMPY and [¹²⁵I]TZDM, respectively, at nanomolar concentrations [120,126].

Kudo and co-workers first evaluated a series of 2-styrylbenzoxazole derivatives on the basis of their binding affinities for A β aggregates, binding selectivity to amyloid plaques (fluorescent staining), and brain uptake *in vivo*, and then selected **89** (BF-168) as a lead compound for amyloid imaging studies. A biodistribution study of [¹⁸F]BF-168 in normal mice showed good initial brain uptake and moderately favorable clearance [130]. However, *ex vivo* autoradiography of [¹⁸F]BF-168 in normal rat indicated slight residual radioactivity in the white matter [128]. Thus, these authors further synthesized and evaluated several derivatives related to BF-168, and then developed an optimal compound, **94** (BF-227), with regard to brain pharmacokinetics.

Replacement of the phenyl ring of BF-168 with a thiazole ring resulted in no change in the binding affinity of this compound for A β aggregates; namely, compound BF-227 exhibited high binding affinities for A β 40 (K_i: 1.5 nM) and A β 42 (K_i: 4.9 nM) [132]. A brain uptake study of [¹¹C]BF-227 demonstrated excellent brain penetration (7.9 %ID/g at 2 min) and rapid clearance from the brain (0.72 %ID/g at 60 min). *In vitro* autoradiography of [¹¹C]BF-227

Table 1. Binding affinities (K_i, nM) of the Ligands with Framework A for A β Aggregates (A β ₄₀ and/or A β ₄₂) or AD Brain Homogenates (AD-BH) and the Log P_{Oct} Values

Compound No		Framework	R ₁	R ₂	R ₃	K _i (nM)	Log P _{Oct}	Amyloid sample	Ref
1	(X-34)	A	CO ₂ H	OH	H	18	0.42	A β ₄₀	[27]
2		A	CO ₂ H	OCH ₃	H	47	-0.95	A β ₄₀	[27]
3		A	CO ₂ H	H	H	135	0.39	A β ₄₀	[27]
4		A	CO ₂ CH ₃	OH	H	119	3.4	A β ₄₀	[27]
5		A	H	OH	OH	9	-	A β ₄₀	[27]
6		A	OH/OCH ₃	OH	H	18	-	A β ₄₀	[27]
7	(Me-X34) ^a	A	CO ₂ H	OH/OCH ₃	H	-	-	A β ₄₀	[98]
8	(MeX04)	A	H	OH	OCH ₃	26.8 ^b , 19.5 ^c	2.6	A β ₄₀	[98, 27]
9	(BSB)	A	CO ₂ H	OH	Br	400	-	A β	[99]
10	(ISB)	A	CO ₂ H	OH	I	0.08 ^d , 0.15 ^c	1.54	A β ₄₀ , A β ₄₂	[100]
11	(IMSB)	A	CO ₂ H	OCH ₃	I	0.13 ^d , 0.73 ^c	0.04	A β ₄₀ , A β ₄₂	[100]
12	(FESB) ^a	A	H	OCH ₃	OCH ₂ CH ₂ F	-	-	-	[101]

^a K_i values were not reported in the references. ^b K_i value for A β ₄₀ aggregates. ^c K_i value for A β ₄₂ aggregates.

Table 2. Binding Affinities (K_i, nM) of the Ligands with Framework B for A β Aggregates (A β ₄₀ and/or A β ₄₂) or AD Brain Homogenates (AD-BH) and the Log P_{Oct} Values

Compound No		Framework	X	Y	R ₄	R ₅	K _i (nM)	Log P _{Oct}	Amyloid sample	Ref
13	(BTA-0)	B	S	N	H	NH ₂	37	2.0 ^a	A β ₄₀	[84]
14	(BTA-1)	B	S	N	H	NHCH ₃	11	2.7 ^a	A β ₄₀	[103, 84]
15	(BTA-2)	B	S	N	H	N(CH ₃) ₂	4.0	3.4 ^a	A β ₄₀	[84]
16		B	S	N	6-CH ₃	NHCH ₃	10	3.1 ^a	A β ₄₀	[103, 84]
17		B	S	N	6-CH ₃	N(CH ₃) ₂	64	3.8 ^a	A β ₄₀	[103, 84]
18		B	S	N	6-OCH ₃	NHCH ₃	4.9	2.6 ^a	A β ₄₀	[84]
19		B	S	N	6-OCH ₃	N(CH ₃) ₂	1.9	3.3 ^a	A β ₄₀	[84]
20	(PIB)	B	S	N	6-OH	NHCH ₃	4.3	1.2 ^a	A β ₄₀	[84]
21		B	S	N	6-OH	N(CH ₃) ₂	4.4	2.0 ^a	A β ₄₀	[84]
22		B	S	N	6-Br	NHCH ₃	1.7	3.6 ^a	A β ₄₀	[84]
23		B	S	N	6-Br	N(CH ₃) ₂	2.9	4.4 ^a	A β ₄₀	[84]
24		B	S	N	6-CN	NHCH ₃	8.6	2.5 ^a	A β ₄₀	[84]
25		B	S	N	6-CN	N(CH ₃) ₂	11	3.2 ^a	A β ₄₀	[84]
26		B	S	N	6-(OCH ₂ CH ₂) ₂ F	NHCH ₃	2.2	3.04	AD-BH	[126]
27		B	S	N	6-(OCH ₂ CH ₂) ₃ F	NHCH ₃	2.8	3.04	AD-BH	[126]
28		B	S	N	6-(OCH ₂ CH ₂) ₆ F	NHCH ₃	4.7	2.99	AD-BH	[126]
29		B	S	N	6-(OCH ₂ CH ₂) ₈ F	NHCH ₃	9.0	-	AD-BH	[126]

(Table 2) Contd....

Compound No		Frame-work	X	Y	R ₄	R ₅	Ki (nM)	Log P _{Oct}	Amyloid sample	Ref
30		B	S	N	6-OCH ₃	OH	4.2	1.8	Aβ ₄₀	[105]
31		B	S	N	6-NO ₂	NHCH ₃	2.75	2.96	Aβ ₄₀	[105]
32		B	S	N	6-NH ₂	OCH ₃	6.9	1.76	Aβ ₄₀	[105]
33		B	S	N	H	F	9	2.76	AD-BH	[115]
34		B	S	N	6-CH ₃	F	5.7	-	AD-BH	[116]
35	(TZDM)	B	S	N	6-I	N(CH ₃) ₂	0.06 ^b , 0.14 ^c	1.84	Aβ ₄₀ , Aβ ₄₂	[100]
36	(TZPI)	B	S	N	6-I	4-methylpiperazin-1-yl	0.13 ^b , 0.15 ^c	2.49	Aβ ₄₀ , Aβ ₄₂	[100]
37	(IBOX)	B	O	N	6-I	N(CH ₃) ₂	0.8	2.09	Aβ ₄₀	[107]
38		B	S	C	H	OCH ₃	0.40 ^d , 0.52 ^e	3.07	Aβ ₄₀ , Aβ ₄₂	[117]
39		B	S	C	H	OH	3.04 ^d , 3.72 ^e	2.99	Aβ ₄₀ , Aβ ₄₂	[117]
40		B	S	C	H	OCH ₂ CH ₂ F	0.67 ^d , 0.87 ^e	2.83	Aβ ₄₀ , Aβ ₄₂	[117]
41		B	S	C	H	OCH ₂ CH ₂ CH ₂ F	0.65 ^d , 0.73 ^e	2.88	Aβ ₄₀ , Aβ ₄₂	[117]
42		B	S	C	H	NH ₂	4.31 ^d , 6.50 ^e	2.87	Aβ ₄₀ , Aβ ₄₂	[117]
43		B	S	C	H	NHCH ₃	0.28 ^d , 0.72 ^e	3.20	Aβ ₄₀ , Aβ ₄₂	[117]
44		B	S	C	H	N(CH ₃) ₂	1.06 ^d , 0.63 ^e	3.44	Aβ ₄₀ , Aβ ₄₂	[117]
45		B	S	C	H	NHCH ₂ CH ₂ F	1.56 ^d , 0.98 ^e	3.46	Aβ ₄₀ , Aβ ₄₂	[117]
46		B	S	C	H	NHCH ₂ CH ₂ CH ₂ F	0.73 ^d , 0.77 ^e	3.56	Aβ ₄₀ , Aβ ₄₂	[117]
47		B	O	C	5-OCH ₃	NH ₂	2.3	-	AD-BH	[108]
48		B	O	C	5-OH	NH ₂	11.5	-	AD-BH	[108]
49		B	O	C	5-OCH ₃	NHCH ₃	1.3	-	AD-BH	[108]
50		B	O	C	5-OH	NHCH ₃	0.7	2.36	AD-BH	[108]
51		B	O	C	5-OCH ₃	N(CH ₃) ₂	12.0	-	AD-BH	[108]
52		B	O	C	5-OH	N(CH ₃) ₂	2.8	-	AD-BH	[108]
53		B	O	C	5-Br	NHCH ₃	2.7	-	Aβ ₄₀	[109]
54		B	O	C	5-Br	OCH ₃	1.3	-	Aβ ₄₀	[109]

^a Log P values determined by reverse phase HPLC methods [84]. ^b Kd (nM) for Aβ₄₀ aggregates. ^c Kd value (nM) for Aβ₄₂ aggregates. ^d Ki value for Aβ₄₀ aggregates. ^e Ki value for Aβ₄₂ aggregates.

Table 3. Binding Affinities (Ki, nM) of the Ligands with Framework C and D for Aβ Aggregates (Aβ₄₀ and/or Aβ₄₂) or AD Brain Homogenates (AD-BH), and the Log P_{Oct} Values

Compound No		Frame-work	X	Y	R ₆	R ₇	Ki (nM)	Log P _{Oct}	Amyloid sample	Ref
55		C	C	-	<i>m</i> -I	N(CH ₃) ₂	4.5	-	Aβ ₄₀	[120]
56		C	C	-	<i>p</i> -I	N(CH ₃) ₂	2.0	-	Aβ ₄₀	[120]
57		C	C	-	<i>p</i> -F	N(CH ₃) ₂	22	-	Aβ ₄₀	[120]
58		C	C	-	<i>p</i> -OCH ₃	NO ₂	151	-	Aβ ₄₀	[122]

(Table 3) Contd....

Compound No		Frame-work	X	Y	R ₆	R ₇	Ki (nM)	Log P _{Oct}	Amyloid sample	Ref
59		C	C	-	<i>p</i> -OCH ₃	NH ₂	36	-	Aβ ₄₀	[122]
60		C	C	-	<i>p</i> -OCH ₃	NHCH ₃	1.2	-	Aβ ₄₀	[122]
61	(SB-13)	C	C	-	<i>p</i> -OH	NHCH ₃	6.0	2.36	Aβ ₄₀	[122]
62		C	C	-	<i>p</i> -OCH ₃	N(CH ₃) ₂	1.3	-	Aβ ₄₀	[122]
63		C	C	-	<i>p</i> -OH	N(CH ₃) ₂	1.2	-	Aβ ₄₀	[122]
64		C	C	-	<i>p</i> -(OCH ₂ CH ₂) ₂ F	NHCH ₃	2.9	2.52	AD-BH	[124]
65		C	C	-	<i>p</i> -(OCH ₂ CH ₂) ₃ F	NHCH ₃	6.7	2.41	AD-BH	[124]
66		C	C	-	<i>p</i> -(OCH ₂ CH ₂) ₄ F	NHCH ₃	4.4	2.05	AD-BH	[124]
67		C	C	-	<i>p</i> -(OCH ₂ CH ₂) ₃ F	NHCH ₃	6.0	2.28	AD-BH	[124]
68		C	C	-	<i>p</i> -OH	NH ₂	95	-	AD-BH	[123]
69		C	C	-	<i>p</i> -OCH ₂ CH(CH ₂ OH)CH ₂ F	NH ₂	15	-	AD-BH	[123]
70		C	C	-	<i>p</i> -OH	N(CH ₃) ₂	1.1	-	AD-BH	[123]
71		C	C	-	<i>p</i> -OCH ₂ CH(CH ₂ OH)CH ₂ F	N(CH ₃) ₂	15	3.13	AD-BH	[123]
72		C	C	-	<i>p</i> -OCH ₂ CH(CH ₂ OH) ₂	N(CH ₃) ₂	38	-	AD-BH	[123]
73	(FMAPO)	C	C	-	<i>p</i> -OCH ₂ CH(CH ₂ OH)CH ₂ F	NHCH ₃	5.0	2.94	AD-BH	[123]
74		C	C	-	<i>p</i> -OCH ₂ CH(CH ₂ OH) ₂	NHCH ₃	32.5	-	AD-BH	[123]
75		C	N	-	<i>p</i> -(OCH ₂ CH ₂) ₃ OH	NH ₂	91.2	-	AD-BH	[127]
76		C	N	-	<i>p</i> -(OCH ₂ CH ₂) ₃ OH	N(CH ₃) ₂	2.2	-	AD-BH	[127]
77		C	N	-	<i>p</i> -(OCH ₂ CH ₂) ₃ F	NH ₂	150	-	AD-BH	[127]
78		C	N	-	<i>p</i> -(OCH ₂ CH ₂) ₃ F	NHCH ₃	10	-	AD-BH	[127]
79		C	N	-	<i>p</i> -(OCH ₂ CH ₂) ₃ F	N(CH ₃) ₂	2.5	3.22	AD-BH	[127]
80		C	N	-	<i>p</i> -Br	NHCH ₃	7.0	-	AD-BH	[125]
81		C	N	-	<i>p</i> -Br	N(CH ₃) ₂	3.2	-	AD-BH	[125]
82		C	N	-	<i>p</i> -I	N(CH ₃) ₂	4.8	1.92	AD-BH	[125]
83	(BF-133)	D	C=C	C	5-F	N(CH ₃) ₂	2.1 ^a , 3.4 ^b	-	Aβ ₄₀ , Aβ ₄₂	[129]
84	(BF-145)	D	C=C	C	5-F	NHCH ₃	3.0 ^a , 4.5 ^b	-	Aβ ₄₀ , Aβ ₄₂	[129]
85	(BF-140)	D	C=C	C	5-F	NH ₂	4.7 ^a , 2.1 ^b	-	Aβ ₄₀ , Aβ ₄₂	[129]
86	(BF-164)	D	C=C	C	6-H	NH ₂	0.38	-	Aβ ₄₂	[130]
87	(BF-169)	D	C=C	C	6-H	NHCH ₃	7.1	-	Aβ ₄₂	[130]
88	(BF-165)	D	C=C	C	6-OH	NHCH ₃	1.8	-	Aβ ₄₂	[130]
89	(BF-168)	D	C=C	C	6-OCH ₂ CH ₂ F	NHCH ₃	2.5 ^a , 6.4 ^b	1.79	Aβ ₄₀ , Aβ ₄₂	[130]
90	(N-282)	D	C=C	C	6-H	N(CH ₃) ₂	4.3	-	Aβ ₄₂	[130]
91	(BF-148)	D	C=C	C	6-F	N(CH ₃) ₂	4.2	-	Aβ ₄₂	[130]
92	(BF-125)	D	C=C	C	6-H	N(CH ₂ CH ₃) ₂	1.5 ^a , 4.9 ^b	-	Aβ ₄₀ , Aβ ₄₂	[130]
93	(BF-180)	D	C=C	C	5-I	N(CH ₃) ₂	6.7 ^a , 10.6 ^b	-	Aβ ₄₀ , Aβ ₄₂	[130]
94	(BF-227)	D	S	N	6-OCH ₂ CH ₂ F	N(CH ₃) ₂	1.8 ^a , 4.3 ^b	1.75	Aβ ₄₀ , Aβ ₄₂	[132]

(Table 3) Contd....

Compound No	Frame-work	X	Y	R ₆	R ₇	Ki (nM)	Log P _{Oct}	Amyloid sample	Ref
95	D	C=C	C	6-(OCH ₂ CH ₂) ₃ F	N(CH ₃) ₂	14.5	2.93	AD-BH	[126]
96	D	C=C	C	6-(OCH ₂ CH ₂) ₆ F	N(CH ₃) ₂	10.0	-	AD-BH	[126]
97	D	C=C	C	6-(OCH ₂ CH ₂) ₈ F	N(CH ₃) ₂	6.0	-	AD-BH	[126]

^a Ki value for Aβ₄₀ aggregates. ^b Ki value for Aβ₄₂ aggregates.

Table 4. Binding Affinities (Ki, nM) of the Ligands with Framework E-L for Aβ Aggregates (Aβ₄₀ and/or Aβ₄₂) or AD Brain Homogenates (AD-BH) and the Log P_{Oct} Values

Compound No	Frame-work	R ₈	R ₉	Ki (nM)	Log P _{Oct}	Amyloid sample	Ref	
98	(FDDNP)	E	C(CN) ₂	-	0.12(H) ^a , 1.86(L) ^b	-	Aβ ₄₀	[136]
99	(FENE)	E	O	-	0.16(H) ^a , 71.2(L) ^b	-	Aβ ₄₀	[136]
100	(IMPY)	F	I	N(CH ₃) ₂	15	2.18	Aβ ₄₀	[110]
101		F	CH ₃	N(CH ₃) ₂	242	-	Aβ ₄₀	[111]
102		F	Br	N(CH ₃) ₂	10.3	-	Aβ ₄₀	[111]
103		F	CH ₃	Br	638	-	Aβ ₄₀	[111]
104		F	N(CH ₃) ₂	Br	339	-	Aβ ₄₀	[111]
105	(FEM-IMPY)	F	I	N(CH ₃)CH ₂ CH ₂ F	27	4.41	Aβ ₄₀	[118]
106	(FPM-IMPY)	F	I	N(CH ₃)CH ₂ CH ₂ CH ₂ F	40	4.60	Aβ ₄₀	[118]
107	(FEPIP)	F	CH ₂ CH ₂ F	N(CH ₃) ₂	177	2.42	Aβ ₄₀	[119]
108	(FPPIP)	F	CH ₂ CH ₂ CH ₂ F	N(CH ₃) ₂	48.3	2.84	Aβ ₄₀	[119]
109		F	(OCH ₂ CH ₂) ₃ F	N(CH ₃) ₂	16	-	AD-BH	[126]
110		F	(OCH ₂ CH ₂) ₂ F	N(CH ₃) ₂	31	-	AD-BH	[126]
111		F	(OCH ₂ CH ₂) ₃ F	N(CH ₃) ₂	30	2.69	AD-BH	[126]
112		F	(OCH ₂ CH ₂) ₆ F	N(CH ₃) ₂	96	-	AD-BH	[126]
113		F	(OCH ₂ CH ₂) ₈ F	N(CH ₃) ₂	387	-	AD-BH	[126]
114		G	OH	OH	4.0	-	AD-BH	[141]
115		G	OH	OCH ₃	6.1	-	AD-BH	[141]
116		G	NH ₂	NH ₂	6.1	-	AD-BH	[141]
117		G	OCH ₃	NO ₂	18.5	-	AD-BH	[141]
118		G	OCH ₃	NH ₂	5.6	-	AD-BH	[141]
119		G	OH	NH ₂	9.6	-	AD-BH	[141]
120		G	OH	N(CH ₃) ₂	7.5	-	AD-BH	[141]
121		G	OCH ₃	NHCH ₂ CH ₂ F	21.5	-	AD-BH	[141]
122		G	OH	NHCH ₂ CH ₂ F	3.9	-	AD-BH	[141]
123		G	OH	NHCH ₃	31.2	-	AD-BH	[141]
124		H	OH	OH	9.0 ^c , 150 ^d	-	AD-BH	[142]